

1 Geochronology of an ultra-long Pleistocene sequence from 2 Kilombe volcano, Kenya

3
4 **S. Hoare¹, J.S. Brink^{2*}, A.I.R. Herries³, D.F. Mark^{4,5}, L.E. Morgan⁴⁺, S.M. Onjala⁶, I.,
5 Rucina⁷, I. Stanistreet^{8,9}, H. Stollhofen¹⁰, J.A.J. Gowlett¹⁺⁺.**

6 1. Archaeology, Classics and Egyptology, HLC, University of Liverpool, L69 3BX, UK

7 2. Florisbad Quaternary Research, National Museum, P.O Box 266, Bloemfontein, 9300,
8 South Africa and Centre for Environmental Management, University of the Free State,
9 South Africa)

10 3. The Australian Archaeomagnetism Laboratory, Dept. Archaeology and History, La Trobe
11 University, Melbourne Campus, Bundoora, 3086, VIC, Australia

12 4. Scottish Universities Environmental Research Centre, Isotope Geosciences Unit, Rankine
13 Avenue, East Kilbride, Scotland, G75 0QF, UK

14 5. Department of Earth and Environmental Science, University of St Andrews, St Andrews,
15 KY16 9AJ, UK

16 6. School of Humanities and Social Sciences, Jaramogi Oginga Odinga University of Science
17 and Technology, P.O. Box 2480-40100 Kisumu, Kenya

18 7. National Museums of Kenya, P.O. Box 40658, Nairobi, Kenya

19 8. Department of Earth, Ocean and Ecological Sciences, University of Liverpool, L69 3BX,UK

20 9. Stone Age Institute, Bloomington, Indiana. 47433, USA

21 10. GeoZentrum Nordbayern, Friedrich-Alexander-University (FAU) Erlangen-Nürnberg,
22 91054 Erlangen, Germany.

23
24 * Deceased

25 + Present address: USGS, Denver Federal Center – MS963, Denver Co80225, USA

26 ++ Corresponding author: email gowlett@liverpool.ac.uk

27
28 Declaration of interests: none

29

30

31

Abstract

We report a new extended stratigraphic sequence with associated Palaeolithic sites from the area of the extinct Kilombe Volcano in central Kenya. The extended archaeological sequence runs from Oldowan finds, through the Acheulean, and up to the Middle Stone Age. The sedimentary sequences within the Kilombe caldera and south flanks of the mountain have been dated through $^{40}\text{Ar}/^{39}\text{Ar}$ measurements and palaeomagnetic studies. A series of $^{40}\text{Ar}/^{39}\text{Ar}$ dates the geological sequence from 2.493 ± 0.095 Ma, near the beginning of the Lower Pleistocene, through to 0.118 ± 0.030 Ma near the Middle to Upper Pleistocene transition. It includes the first entirely new Oldowan localities in East Africa for thirty years, and the first in a rugged mountain environment. Eruptions of trachyte lavas of Kilombe mountain took place during and after c. 2.5 Ma, followed by a sequence of bedded tuffs, diamictites, sandstones, and claystones. Sections in the mid part of this intra-caldera sequence have produced dates of 1.8 - 1.7 Ma, associated with an Oldowan industry and fauna, overlain by Acheulean finds. On the southern outward flanks of Kilombe mountain, a second major sequence is bounded at the base by trachyphonolite dated c. 1.6 Ma. The main Acheulean archaeological site (GqJh1) falls within the overlying sedimentary sequence and has an age of c. 1.0 Ma, on the basis of a new $^{40}\text{Ar}/^{39}\text{Ar}$ date and palaeomagnetic reversal stratigraphy, and $^{40}\text{Ar}/^{39}\text{Ar}$ dates indicate an age of c. 0.46-0.48 Ma for a marker ashflow tuff (AFT), prominent across the area. At Moricho, W of Kilombe, sediments above the AFT have been dated in the range 270,000 – 120,000 years and are associated with Middle Stone Age assemblages. In total, these sites attest to hominin activity from an Oldowan horizon dated to 1.814 ± 0.004 Ma up to LSA stone scatters within the last 100,000 years.

55

56

KEYWORDS; Argon-Argon Dating; Palaeomagnetism; Acheulean; Oldowan; Large Cutting Tools; Bifaces; Rift Valley

59

60 1. Introduction

61 We report here new research on and around the extinct Kilombe Volcano within the central
62 Rift Valley of Kenya (Figures 1A, 1B). The results include the discovery of new traces of
63 hominin activity within the Kilombe caldera, description of the stratigraphic sequence, and a
64 series of $^{40}\text{Ar}/^{39}\text{Ar}$ dates which show the sequence spans the entire Pleistocene. The area has
65 previously been best known for its Acheulean archaeology, and its setting of major explosive
66 volcanic centres such as Menengai and Londiani (Bishop 1978; Blegen et al. 2016; Gowlett
67 1978, 1993; Gowlett et al. 2015, 2017; McCall 1964, 1967; Jennings 1971; Jones 1975, 1985;
68 Jones and Lippard 1979). There are two principal volcanic settings: the fill of the Kilombe
69 caldera, and the southern flanks of the Kilombe volcanic cone (Figure 2).

70 1.1 Kilombe Volcano and surrounding area

71 Kilombe mountain is an extinct trachytic volcano, located at the western side of the eastern
72 branch of the East African Rift System (EARS) (Figures 1A, 1B), and exposes mainly trachyte
73 lavas and volcanoclastic sediments: its cone is about 20 km across, and it stands to heights of
74 ~2300 m asl. On the south side, the Molo river descends from the Mau escarpment and passes
75 around the southern edge of the mountain. The river eventually flows northwards into Lake
76 Baringo, which is part of the internal drainage system. The northern side of the volcano has
77 few exposures and is not yet explored. The extinct trachytic volcano comprises a caldera about
78 3 km in diameter, which is now drained by a stream running out through a gorge on the eastern
79 side of the mountain. Erosional downcutting has exposed a series of sedimentary rocks and
80 interleaved tuffs of the intra-caldera fill. A waterfall marks the rapid descent from the caldera
81 through the deepest part of the gorge (Figures 2, 4.; waterfall location, Figure 5), and in its cliff
82 a massive tuff and a trachytic lava flow, interleaved with underlying lacustrine sediments are
83 identified, representing the oldest part of the exposed Kilombe caldera-fill.

84 The geology of the Kilombe caldera was originally studied and mapped by McCall (1964,
85 1967), and the wider area subsequently by Jennings (1971) and Jones (1975, 1985, 1988; Jones
86 and Lippard 1979), the latter working within the extensive East African Geological Research
87 Unit (EAGRU) project during the 1970s. Acheulean sites have been known on the southern
88 flank of Kilombe mountain since the 1970s (Bishop 1978; Gowlett 1978) and are the subject
89 of continuing study (Gowlett et al. 2015, 2017).

90 Our recent research has greatly expanded the range of known geological and archaeological
91 contexts on Kilombe Volcano, both within and outside the caldera. In this paper we describe
92 the newly encountered intra-caldera sequence and associated early archaeological (Oldowan
93 and Acheulean) and faunal localities; as well as additional exposures around the southern
94 flanks, especially towards the west at Moricho, where the Middle Stone Age is best
95 characterized and dated.

96 **1.2 New research and an outline succession**

97 Prior to the current research, there was only a low-precision chronological framework for some
98 of the main volcanic events in the area, provided by $^{40}\text{K}/^{40}\text{Ar}$ ages. These data indicated lower
99 Pleistocene volcanic activity, and recurrent hominin activity in the Middle Pleistocene (Jones
100 and Lippard 1979). Two palaeomagnetic datum points were obtained for the three-banded tuff
101 on the Kilombe Acheulean Main Site in the 1970s (Dagley et al. 1978; Gowlett 1978, p. 225).
102 They have been checked and added to in recent and ongoing work (Herries et al. 2011).

103 The age of trachytic lavas of Kilombe mountain temporally constrain the base of the sequence
104 outcropping in the area (Figure 3). The trachyte of the caldera rim separates two different
105 sequences of sediment. One sequence is contained within the caldera and starts with exposures
106 below the base of the waterfall in the gorge (Figure 5). This caldera-fill sequence can be traced
107 upwards in two exposure, termed here by analogy ‘staircases’, which we define here as the
108 *upper staircase*, running within the caldera up to a height of ca. 2050 m (Figures 4, 5); and the
109 *lower staircase*, which runs within the gorge, descending along the edge of a small side gorge
110 and continuing right down to the waterfall and the stream in the base of the gorge (Figures 4,
111 5). Together these exposures preserve a sequence of more than 130 m thick. The sections
112 exposed in the staircases belong almost entirely to the early Pleistocene, as do newly discovered
113 Oldowan and Acheulean archaeological occurrences introduced below; Middle Pleistocene
114 sediments however overlie unconformities in the caldera valley and gorge.

115 The other, largely younger, sequence is exposed on the outer southern slopes of Kilombe
116 Volcano (Figs 2, 3). Trachyphonolite lava forms a spur that projects southwards towards the
117 Molo River and is topped by an erosion surface. This trachyphonolite lava underlies most of
118 the archaeologically significant sequences outside the volcano, which are exposed mainly in a
119 series of gullies started by minor streams running off the eastern side of the spur, and eventually
120 joining with the Molo River several kilometres downstream. The lava appears to be coeval
121 with and correlate to the series of trachyphonolites that include the Lake Hannington

122 Trachyphonolite (McCall 1964, 1967; Jones 1975, 1985), and are extensive in the rift valley
123 floor to the north of the sites (Griffiths and Gibson 1980). At Kilombe the trachyphonolite is
124 widely overlain by a series of generally reddish sediments, including tuffs. First in the
125 sequence, immediately above the trachyphonolite, come brown and red claystones which have
126 been interpreted as weathering products of the lavas (Bishop 1978). The Acheulean Main Site,
127 GqJh 1 (Figure 2) known since the 1970s lies at the top of these, within a local broad, shallow
128 clay-filled gully (Bishop 1978; Gowlett 1978; Gowlett et al. 2015, 2017). Above the site level
129 comes the Three-banded tuff (3BT), overlain by a sequence of ca 15 metres of reddish tuffs,
130 claystones, sandstones and siltstones (the Farmhouse cliff sediments), capped by a massive ash
131 flow tuff (the AFT – see below). This tuff marks the beginning of the series of sediments
132 assigned to the “Menengai Assemblage” by Jones (1975), mainly made up by reddish
133 sediments and tuffs up to a thickness of 15-30 metres. These were named the Esageri Beds by
134 Jones, and are best exposed at Moricho (Figures 2, 3), 2 km west of the Kilombe Main Site
135 (GqJh1), and in large gully systems to the east of the research area (Figure 2).

136 In an area within a radius of 3 km from the Acheulean Main Site (GqJh1), and extending along
137 the southern lower flanks of Kilombe mountain north of the Molo River (Figure 2), further
138 Acheulean sites have now been located within the Farmhouse Cliff sediments (Gowlett et al.
139 2015), at higher stratigraphic levels than the GqJh1 site. Middle (MSA) and Later Stone Age
140 (LSA) occurrences have also been found above the AFT within the Esageri Beds, especially at
141 Moricho (Gowlett et al. 2015). They demonstrate that the Kilombe mountain flank sequence
142 offers the potential to elucidate changes in lithic technology over nearly a million years,
143 including the transition from the Acheulean to MSA, as also seen to the north in the Kapthurin
144 Formation (McBrearty 1999; Johnson and McBrearty 2010; Tryon and McBrearty 2002), and
145 to the south at Olorgesailie (Brooks et al. 2018; Deino et al. 2018).

146

147 **2. Methods**

148 **2.1 Survey**

149 Survey has been carried out across the Kilombe mountain flank in continuation from previous
150 studies, using standard map recording methods, aided by GPS and satellite imagery and
151 photography. Sections around the Main Site (GqJh1) and in the caldera have been measured
152 by laser theodolite at <5cm vertical accuracy. Archaeological sites were given designations

153 using the standard SASES naming system in accordance with National Museums of Kenya
154 registration practice.

155 **2.2 Sample Collection for $^{40}\text{Ar}/^{39}\text{Ar}$ geochronology**

156 Samples of tuffs and lava flows were collected during field seasons from 2011-2017. Samples
157 were taken from primary volcanic deposits as defined by Bishop (1978), except for the intra-
158 caldera volcanoclastics (Kil 2-4 and 2-8) samples, which included both primary tuff and lahar
159 deposits. Fresh material for all the samples was extracted following removal of surface
160 contamination and any weathered material. Each location was recorded using a handheld GPS
161 unit and named according to Bishop's (1978) lithostratigraphy, aside from Kil 2-7.

162 **2.3 Sample preparation and $^{40}\text{Ar}/^{39}\text{Ar}$ geochronology**

163 A detailed sample preparation routine is discussed by Mark et al. (2010; 2014) but briefly:
164 feldspars (sanidine) were separated after disaggregating, washing and sieving followed by
165 magnetic and density separations and finally ultrasonic cleaning in 5% hydrofluoric acid for 5
166 min. Feldspars were handpicked under binocular microscope for analysis. Samples were
167 irradiated in the CLICIT facility of the Oregon State University TRIGA reactor using the Alder
168 Creek sanidine as a neutron fluence monitor.

169 $^{40}\text{Ar}/^{39}\text{Ar}$ analyses were conducted at the NERC Argon Isotope Facility, Scottish Universities
170 Environmental Research Centre (SUERC). Details of irradiation durations, J measurements,
171 discrimination corrections are provided in appendix file DM1. Irradiation correction
172 parameters are shown below.

173 For J determinations three bracketing standard positions surrounding each unknown were used
174 to monitor the neutron fluence. Eight measurements were made for each bracketing standard
175 position. The weighted average $^{40}\text{Ar}^*/^{39}\text{Ar}_K$ was calculated for each well, and the arithmetic
176 mean and standard deviation of these three values was used to characterize the neutron fluence
177 for the unknowns. This approach was deemed sufficient as, due to the relatively short
178 irradiation durations, there was no significant variation between the three positions in a single
179 level of the irradiation holder. This also facilitated high-precision measurement of the J-
180 parameter. Note that for all J-measurements no data were rejected.

181 Samples were analyzed in several batches. Air pipettes were run (on average) after every 5
182 analyses. Backgrounds subtracted from ion beam measurements were arithmetic averages and

183 standard deviations. Mass discrimination was computed based on a power law relationship
184 (Renne et al. 2009) using the isotopic composition of atmospheric Ar reported (Lee et al. 2006)
185 that has been independently confirmed (Mark et al. 2011). Corrections for radioactive decay of
186 ^{39}Ar and ^{37}Ar were made using the decay constants reported by Stoenner et al. (1965) and
187 Renne and Norman (2001), respectively. Ingrowth of ^{36}Ar from decay of ^{36}Cl was corrected
188 using the $^{36}\text{Cl}/^{38}\text{Cl}$ production ratio and methods of Renne et al. (2008) and was determined to
189 be negligible. Argon isotope data corrected for backgrounds, mass discrimination, and
190 radioactive decay and ingrowth are given in the appendix file DM1 (.pdf).

191 The samples were analyzed by total fusion with a CO_2 laser and measurements made using a
192 MAP 215-50 (MAP2) noble gas mass spectrometer. The mass spectrometer is equipped with a
193 Nier-type ion source and analogue electron multiplier detector. Mass spectrometry utilized
194 peak-hopping by magnetic field switching on a single detector in 10 cycles.

195 Ages were computed from the blank-, discrimination- and decay-corrected Ar isotope data after
196 correction for interfering isotopes based on the following production ratios, determined from
197 fluorite and Fe-doped KAlSiO_4 glass: $(^{36}\text{Ar}/^{37}\text{Ar})_{\text{Ca}} = (2.650 \pm 0.022) \times 10^{-4}$; $(^{38}\text{Ar}/^{37}\text{Ar})_{\text{Ca}} =$
198 $(1.96 \pm 0.08) \times 10^{-5}$; $(^{39}\text{Ar}/^{37}\text{Ar})_{\text{Ca}} = (6.95 \pm 0.09) \times 10^{-4}$; $(^{40}\text{Ar}/^{39}\text{Ar})_{\text{K}} = (7.3 \pm 0.9) \times 10^{-4}$;
199 $(^{38}\text{Ar}/^{39}\text{Ar})_{\text{K}} = (1.215 \pm 0.003) \times 10^{-2}$; $(^{37}\text{Ar}/^{39}\text{Ar})_{\text{K}} = (2.24 \pm 0.16) \times 10^{-4}$, as determined
200 previously for this reactor in the same irradiation conditions (Renne 2014). Ages and their
201 uncertainties are based on the methods of Renne et al. (2010), the calibration of the decay
202 constant as reported by Renne et al. (2011) and the ACs optimization age (1.1891 ± 0.0009
203 Ma, 1 sigma) as reported by Niespolo et al. (2017), except where noted. The optimization-
204 modeled age for the ACs standard has accurate quantifiable uncertainties and hence is favoured
205 here over the astronomically tuned ACs age presented by Niespolo et al. (2017). The reason
206 for this is that the astronomical calibration has unknown uncertainty and confidence intervals
207 and uses best guess ‘assumptions’ to constrain, for example, phase relationships between
208 insolation and climate within the Pleistocene.

209

210 **3. Results**

211 **3.1 $^{40}\text{Ar}^*/^{39}\text{Ar}$ Dates**

212 17 samples were $^{40}\text{Ar}^*/^{39}\text{Ar}$ dated in tota and the geochronological data and plots are presented
213 in Appendix File DM1. Age computation uses the weighted (by inverse variance) mean of

214 $^{40}\text{Ar}^*/^{39}\text{Ar}_K$ values for the sample and standard, combined as R -values and computed using the
215 method of Renne et al. (2010). Outliers in both single-crystal samples and standards were
216 discriminated using a 3-sigma filter applied iteratively until all samples counted are within 3
217 standard deviations of the weighted mean \pm one standard error. This procedure screened older
218 crystals that are logically interpreted as xenocrysts. Some young crystals were rejected on the
219 basis of low radiogenic ^{40}Ar yields due to analysis of exceptionally small or low-K crystals or
220 as statistical flyer. Processing of the data using the $n\text{MAD}$ approach of Kuiper et al. (2008)
221 has no impact on the probability distribution plots for each sample. All ages are reported as X
222 $\pm Y$ where Y includes all sources of uncertainty as determined through the optimization
223 approach of Renne et al. (2010), using the parameters of Renne et al. (2011), and the standard
224 age of Niespolo et al. (2017). The $^{40}\text{Ar}/^{39}\text{Ar}$ dates are summarised in **Table 1**. Further data are
225 provided in supplementary data file DM1. Below we present in more detail the new
226 stratigraphic framework, archaeological occurrences and their relationship with chronological
227 measurements.

228 **Table 1: Summary of $^{40}\text{Ar}/^{39}\text{Ar}$ data. Descriptions of each individual age are recorded in**
229 **supplementary file DM1.**

230

Sample-ID	Age (Ma) ± Ma (1s)	Sampled layer	Polarity	Palaeomag. Constraint
<i>Mountain Flank</i>				
Kil 2-1	0.111 0.020	Top Seq. Tuff		
Kil 2-7	0.127 0.030	MSA 200		
Kil 3-5	0.266 0.003	Moricho Tuff 105		
Kil 3-4	0.275 0.011	Moricho Tuff 104		
Kil 3-3	0.248 0.004	Moricho Tuff 103		
Kil 1-3	0.461 0.014	AFT	N	<0.78 Ma (Brunhes Chron)
Kil 1-4	0.487 0.011	AFT	N	<0.78 Ma (Brunhes Chron)
Kil 2-2	1.032 0.025	3BT	R	<0.99 Ma (Jaramillo Chron)
Kil 2-5	1.509 0.034	Tuff with grass prints		
Kil 1-2	1.559 0.007	Trachyphonolite		
Kil 1-1	1.580 0.008	Trachyphonolite		
<i>Caldera Sequence</i>				
Kil 1-5	0.469 0.016	Tuff at Waterfall	N	<0.78 Ma (Brunhes Chron)
Kil 2-4	1.761 0.020	Tuff in Caldera GqJh14		
Kil 2-8	1.762 0.022	Tuff in Caldera GqJh13A		
Kil 3-2	1.814 0.004	Tuff in Caldera GqJh12A		
Kil 2-6	2.552 0.038	Trachyte flow base of gorge		
Kil 3-1	2.493 0.009	Trachyte flow Caldera rim		

All ages calculated using the decay constants of Renne et al., 2011

Ages referenced against the Alder Creek sanidine age of Niespolo et al., 2017 (optimization, 1.1891 Ma)

Age calculations used the atmospheric $^{40}\text{Ar}/^{36}\text{Ar}$ of 298.56 ± 0.31 (Lee et al., 2006; Mark et al., 2010)

All ages include systematic uncertainty as calculated using the optimization model of Renne et al., 2010

Polarity: N = normal and R = reversed

231

232

233 3.2 Geochronology and Archaeological relationships

234 The succession is discussed here in ascending chronological order, (i) in the caldera, and (ii)
 235 on the southern flanks of the mountain (Table 1; Figs 2, 3). As far as can be determined all
 236 dates fit in order within the stratigraphic sequence, within the ranges of reported 1-sigma
 237 uncertainty.

238 3.2.1 The mountain and caldera sequence Kilombe mountain trachyte

239 The two earliest dates in the series are derived from trachyte flows of the Kilombe volcanic
 240 cone. Sample Kil 2-6 was selected from the eastern side of the volcano at the foot of the gorge
 241 (Figure 2), and represents the furthest flow of lava to the east of the mountain, with an age of
 242 2.552 ± 0.038 Ma. Sample Kil-3-1 comes from the caldera rim (Figures 2, 5), caldera rim
 243 section, GPS Loc. 140), immediately to the south of the gorge. The position is high on the
 244 mountain and had been interpreted by Jones (1975) as the most recent flow. The age of 2.493

245 ± 0.009 Ma is the oldest in the entire series of $^{40}\text{Ar}/^{39}\text{Ar}$ ages reported here. From the positions
246 of the samples Kil-2-6 and Kil-3-1, it is likely that most of the trachyte flows making up the
247 mountain are somewhat older than ca. 2.4 Ma.

248 The $^{40}\text{Ar}/^{39}\text{Ar}$ ages of ca. 2.4-2.5 Ma are older than the single earlier age determination reported
249 by Jones and Lippard (1979): their sample (14/1) gave a ^{40}K - ^{40}Ar age of 1.90 ± 0.15 Ma.
250 Coordinates which they provided for that sample are 35.50E/00.03S, indicating a point on the
251 northern side of Kilombe Volcano, about 3-4 km NW of our sampling points (Figure 2, sample
252 14/1). There are two potential scenarios to explain the age difference: (1) incomplete extraction
253 of radiogenic ^{40}Ar during laboratory heating may have caused an artificially young age
254 constraint, or (2) that sample maybe from a unit younger than those sampled herein. In total,
255 Jones (1975) recognised more than 13 individual volcanic events. The larger Londiani
256 Volcano, a few km to the west of Kilombe (Figure 1B), is a similar trachyte volcano (Jennings
257 1971), and provided a ^{40}K - ^{40}Ar age of 3.1 ± 0.1 Ma (Jones and Lippard 1979). These results
258 are consistent with the interpretation first set forward by Jennings and Jones that Londiani
259 volcano was active in the late Pliocene, and Kilombe was a centre of volcanic activity during
260 the earliest Pleistocene.

261 3.2.1.2 Kilombe caldera sequence

262 The caldera-fill sequence rises to a height of ca 2 km, just below the summit of the collar of
263 the volcano, and most probably extends over the entire caldera diameter of ca. 3 km (McCall
264 1967; Jennings 1971) (Figures 2, 4). The sediments covering approximately 10 km^2 are largely
265 covered by vegetation but are accessible close to the surface and are exposed in a number of
266 outcrop areas. The caldera fill comprises a series of horizontally bedded tuffs (see also Ridolfi
267 et al. 2006) and massive volcanoclastic breccia and sandstones, interbedded with claystones,
268 thin sandstones and siltstones. This sequence is currently best exposed in a trackway ascending
269 from a dammed pool in the caldera centre, comprising the *upper staircase* sequence (Figures
270 5, 6). Deeper portions of the caldera-fill are exposed in a *lower staircase* (Figure 4) descending
271 into the gorge, and lead down to and below the waterfall section. Running from East to West,
272 the entire set of exposures in the *upper staircase* rises 100 m along a length of ca. 500 m. The
273 *lower staircase* runs approximately SSW to NNE along 250 m, descending from ~1980 to
274 ~1920 m (Figure 4).

275 The first fossil bones from the sequence were found by the farmer Mr Philip Kogai during the
276 digging of a latrine pit at a level near the base of the upper staircase section (This is confirmed

277 to be the same level explored in site GqJh 13A, which is a few m south of the latrine: Figure
278 5). In a striking case of research impact, stimulated by knowledge of investigations in the area
279 outside the volcano he reported the bones to the Museums, and they were confirmed as
280 representing mineralised fossil material contained within a volcano-sedimentary unit.

281 The well-preserved fossils found subsequently in the upper staircase sequence, include extinct
282 bovids and hippopotamus identified by JB as *Hippopotamus gorgops*. Since 2012 road
283 improvements to the trackway have obscured the view of stratigraphy, but it has been possible
284 to clean new sections in the side of the road, and to identify within the staircase many
285 successive tuffs, volcanoclastic sandstones and diamictites resulting from lahars (volcanically
286 related mudflows), separated by claystone units, which include siltstone and sandstone
287 interlayers. The many tuffs indicate recurrent eruption of probably more than one nearby
288 (proximal) to distal volcanic sources, and the lahars indicate mudflows reworking material
289 within the confines of Kilombe caldera itself. Individually units are 20 cm up to 100 cm thick,
290 and separated by units of claystone, which exhibit a “waxy” texture (cf Hay 1976:42), related
291 to smectite content, indicative of deposition in a saline-alkaline lake.

292 Two of our $^{40}\text{Ar}/^{39}\text{Ar}$ dated samples relate to the original bone finds in the context of the upper
293 staircase section, and to discoveries made more recently along the road section (site GqJh13A).
294 The ages are 1.761 ± 0.020 Ma for sample Kil-2-4, a tuff about 15 m higher than the finds, and
295 1.762 ± 0.022 Ma for sample Kil-2-8, a thin tuff immediately underlying the bone finds
296 (Figures 3, 4, 5 staircase section). The two dates directly constrain the archaeological and
297 faunal finds in this immediate area and are consistent with the identification of *H. gorgops* in
298 the assemblage. About 30 m of sedimentary sequence overlies the upper dated horizon,
299 culminating in a fairly horizontal surface running across the central part of the caldera.

300 With further help from the farmer, Mr Philip Kogai, we were able to locate and investigate a
301 additional fossil locality about 200 m north of the finds just described (site GqJh12A). A tuff
302 sample Kil 3-2 taken here yields a precise $^{40}\text{Ar}/^{39}\text{Ar}$ age of 1.814 ± 0.004 Ma. Hippopotamus
303 and bovids are represented at this locality, embedded within the tuffaceous sequence.

304 The two $^{40}\text{Ar}/^{39}\text{Ar}$ ages for Kil 2-4 and Kil 2-8 are in stratigraphic order, but considering their
305 uncertainties they are statistically indistinguishable. Together with the $^{40}\text{Ar}/^{39}\text{Ar}$ age for Kil-
306 3-2 they demonstrate an Early Pleistocene age for the fossil localities, approximately
307 contemporary with the part of the sequence at Olduvai including the Bed I/Bed II boundary
308 (Hay 1976; Blumenschine et al. 2003; Deino 2012; Stanistreet et al. 2018). The precise age for

309 Kil 3-2 specifies the bone assemblage here as slightly older than Tuff IF at Olduvai in topmost
310 Bed I.

311 Small numbers of artefacts have been found from three localities at these levels. Their
312 significance is discussed further below. They are Oldowan-like in general character, and
313 mainly made of trachyte. A large core was also found at an isolated exposure on the south side
314 of the gorge, at an elevation of ~ 1985 m. At locality GqJh13A, at the base of the lower
315 staircase, there is proof of multiple bones *in situ*, associated with stone finds (Figure 7).

316 The upper staircase ascends approximately 40 metres along a length of 200 metres, and is
317 mainly composed of a series of interbedded mudflows and tuffs. Towards the top is a series
318 of mudflow units. These contain artefacts of undoubted Acheulean character, including several
319 bifaces and biface flakes. Artefacts are found scattered within the mudflows and are also found
320 concentrated at one interface in a clayey lens. All the main elements of early Acheulean
321 assemblages are represented, including ~6 bifaces, several cores and probable heavy-duty
322 scrapers, and a number of flakes (Figure 8). Some flakes indicate simple working of a core,
323 but one is interpreted as a handaxe trimming flake. Significance of these finds is discussed
324 further below. Further Acheulean finds in the caldera were made in 2019 and the complete
325 assemblages will be reported on separately.

326 3.2.1.3 *The lower staircase and gorge development*

327 Tuffs and other sediments can also be traced at lower levels in the gorge leading out of the
328 caldera. They can be followed in the *lower staircase* (Figures 4, 5) which descends along the
329 western face of a small side gorge on the south side of the main gorge, and then along the spur
330 between the side gorge and main gorge down to the level of the stream. Exposures can also be
331 traced westward intermittently along the south side of the main gorge to the point where it
332 terminates with a vertical rock face, over which the stream descends around 25 metres in the
333 waterfall. At the waterfall a far later massive tuff unconformably overlies horizontal thinly
334 laminated deposits which are lacustrine, in places displaying ripple marks. These and
335 underlying lacustrine sediments appear to be stratigraphically the oldest exposed levels of the
336 caldera fill sequence. A trachyte lava unit at a slightly higher level is interbedded with that
337 oldest sequence, probably recording the last event in the history of the activity of Kilombe
338 Volcano itself. Further dating and palaeomagnetic studies may give added chronological
339 resolution to events between the early lavas at ca 2.5 Ma and the dated tuffs at ca 1.8 Ma.

340 Within the caldera area modern streams cut down through the caldera-fill, joining to make the
341 modern gorge. However there have been earlier phases of gorge development. At the waterfall
342 a proto-gorge incises deeply through the older caldera-fill sequence and this incision is filled
343 by a thick coarse lapilli ash tuff Kil 1-5 which has been $^{40}\text{Ar}/^{39}\text{Ar}$ dated at its base to $0.469 \pm$
344 0.016 Ma (Figure 5).

345 This Middle Pleistocene age shows that the tuff is far younger than all the tuffs and interleaved
346 lacustrine units just described. We deduce that the pronounced unconformity, on which the tuff
347 sits, cuts down deeply through the older sequence. The lacustrine sequence underlying the
348 massive tuff exhibits reversed magnetisation (thus an age >790 ka based on the date of the
349 Brunhes Matuyama transition: Mark et al. 2017), whereas the sequence above and including
350 the tuff exhibits normal polarity, emphasizing the magnitude of the erosional break at the base
351 of the tuff. Jones (1975; also Bishop 1978) identified an Ash Flow Tuff (AFT) in the region
352 which he placed as the basal of unit of his Menengai Series, since he linked the sediments with
353 the earliest eruptions of Menengai (or a proto-Menengai in his terms). Menengai volcano lies
354 about 20 km south of Kilombe, and the tuffs are more thickly developed approaching it from
355 the north side (Jones 1975). The Ash Flow Tuff occurs extensively on the southern flanks of
356 Kilombe, and was also mapped by Jones as occurring in the calderas of Londiani and Kilombe:
357 in 2018 it was observed on the north side of the stream channel within Kilombe Caldera. The
358 date of the incision-fill tuff in the gorge is statistically indistinguishable from those for the Ash
359 Flow Tuff (see below), and we correlate them provisionally. In 2018 exposures of AFT were
360 also found in the caldera on the north side of the valley leading into the top of the gorge.

361 In places lower down the stream course within the gorge remnants of tuffs and mudflows are
362 visible. From this evidence it seems likely that a stream was already draining the caldera and
363 cutting through caldera-fill sediments that were deposited during the Matuyama Chron prior to
364 ca. 470 ka.

365 In summary, the current research has established the presence of extensive early Pleistocene
366 sediments within Kilombe caldera, and temporally constrained them to between ca. 2.4 and 1.7
367 Ma, with extensions to that time range possible. Previously the entire caldera-fill was mapped
368 by Jennings (1971) and Jones (1975) as far younger sedimentation. It is now possible to state
369 with certainty that two different units are involved, separated by a considerable time interval.
370 The bedded tuffs are far older than the massive tuff, which has an age indistinguishable from
371 that of the AFT outside the caldera (see below dates Kil 1-3 and 1-4). The late Pleistocene

372 Menengai tuff (Jones 1975; Blegen et al. 2016, Blegen 2017) is also present within the caldera
373 to the south of the main drainage way.

374 3.2.2. *The succession on the southern mountain flanks*

375 3.2.2.1 *Basal trachyphonolite*

376 On the southern side of the Kilombe Volcano, the Pleistocene sediments cover an area of at
377 least 6 x 3 km, mantling its lower slopes (Figure 2). At the base is a greenish-grey, feldspar-
378 phytic, trachyphonolite lava (Bishop 1978), in places flow-laminated, which forms a spur
379 extending from the south side of the mountain. Although it is largely covered by younger
380 sediments, the trachyphonolite is widespread and exposed in many places, and usually has an
381 irregular undulating surface. A direct stratigraphic relationship with the trachytes of Kilombe
382 mountain has not been observed (Bishop 1978; Jones 1975), but it is certainly less altered. It
383 has yielded two dates at localities about 1 km apart, the first close to the archaeological Main
384 Site (GqJh1), and the second at the Kapsigat road junction nearer to Kilombe mountain (Figure
385 2). They are 1.580 ± 0.008 Ma (Kil-1-1) and 1.559 ± 0.007 Ma (Kil-1-2) respectively. The two
386 $^{40}\text{Ar}/^{39}\text{Ar}$ are statistically indistinguishable. A previous ^{40}K - ^{40}Ar age on the trachyphonolite
387 published by Jones and Lippard (1979) had given the age of 1.70 ± 0.05 Ma (their sample
388 14/369). Its coordinates 35.52E/00.09S (Jones and Lippard 1979) put the sampling point close
389 to the Molo River about 2 km NE of Rongai, and some kilometres SW of our research area.

390 As noted above, no contact has been detected between the trachyphonolite and the trachytes of
391 Kilombe mountain (Bishop 1978; Jones and Lippard 1979), and the stratigraphic relationship
392 has been unclear. Jones (1975) correlated them to the Lake Hannington Trachyphonolite. The
393 new $^{40}\text{Ar}/^{39}\text{Ar}$ dates show that the trachyphonolite substantially postdates the trachytes of
394 Kilombe Volcano itself, and substantially altered the landscape.

395 The new trachyphonolite ages provide the earliest timings for the archaeological and
396 environmental sequence on the southern flanks of Kilombe mountain. It is worth noting that
397 they are also similar to ages for lavas at the base of the Kapthurin Formation 70 km to the north,
398 which are dated at ~ 1.57 Ma. (Deino and McBrearty 2002; McBrearty 1999 Tryon and
399 McBrearty, 2002), and represent part of the same general set of volcanic lava outputs within
400 the Rift.

401 The trachyphonolite lavas outcrop at the present surface in substantial outcrops, but are usually
402 overlain by several metres of red and brown claystones, occasionally containing faunal remains

403 (Bishop 1978; Brink in Gowlett et al. 2015), and which have been previously interpreted to
404 represent accumulated weathering products from the basal lavas (Bishop 1978). Bishop noted
405 a yellowish fine bedded tuff with grass prints occurring within the brown clays on the
406 Acheulean Main Site (GqJh1). This is about 1.5 metres below the main artefact horizon and
407 has now been dated to 1.509 ± 0.034 Ma (Kil-2-5).

408 3.2.2.2 The Acheulean Main Site (GqJh1) and Three-Banded Tuff (3BT)

409 The Acheulean Main Site GqJh 1 (Figures 2, 3) is exposed in an ancient broad shallow gully
410 close to the top of the claystones. The Three-banded tuff (3BT) (named by Bishop 1978) then
411 occurs as a widespread marker on the eastern side of the trachyphonolite spur mentioned above.
412 The 3BT is located about 1 m higher in the sequence than the main Acheulean archaeological
413 horizon and comprises three tabular ash fallout layers, each approximately 30 cm thick.

414 The 3BT was previously suggested to record a reversed magnetic polarity, indicating that the
415 main Acheulean site layer (GqJh1) was older than the age of the Brunhes-Matuyama boundary
416 (Bishop 1978; Gowlett 1978). However, Dagley et al. (1978) were cautious on this point
417 because the three samples were very strongly magnetised, and possibly represented an IRM
418 induced by a lightning strike. The two samples from AH excavation were certainly reversed,
419 but one from EH excavation gave a westerly direction. Our more recent measurements of the
420 3BT confirm that the high magnetisation, along with a reversed polarity, occurs at a number of
421 different exposures of the 3BT spread over hundreds of metres. These findings indicate that
422 the high magnetisation does not result from a lightning strike. The $^{40}\text{Ar}/^{39}\text{Ar}$ age from a sample
423 of the 3BT taken from the main site area is 1.032 ± 0.025 Ma (Kil 2-2).

424 On the basis of the reversed polarity and the new $^{40}\text{Ar}/^{39}\text{Ar}$ age, the 3BT is likely to have formed
425 shortly before or after the Jaramillo Subchron which extends from 1.072-0.988 Ma (Ogg,
426 GTS2012, Chapter 5). Below the 3BT and the archaeological horizons the basal claystones
427 record a normal polarity that may be the Jaramillo Subchron itself. This would suggest that the
428 3BT is somewhat younger than the Jaramillo Subchron, with an age between the upper reversal
429 of that Subchron at 0.988 Ma and the younger limit on the age of date Kil-2-2 on the 3BT of
430 0.982 Ma. At 2 sd (Herries et al. 2011; Gowlett et al. 2015). Alternatively, the main horizon
431 age could be slightly older than Jaramillo, Work on other deposits and a refinement of the
432 reversal that exists between the claystones and the 3BT is ongoing. Within uncertainty, the
433 $^{40}\text{Ar}/^{39}\text{Ar}$ age for this unite fits exactly and suggests that the 3BT was erupted very soon after
434 the archaeological layer was deposited.

435 Durkee and Brown (2014) used correlations of volcanic ashes dating to 992-974 ka to refine
436 the chronology of three other major Acheulean site complexes in Kenya – Olorgesailie, Isinya
437 and Kariandusi. Their correlations suggest that the Kilombe main site (GqJh 1) (Figures 2, 3)
438 may be slightly older than the Kariandusi sites, and the group of Acheulean sites in Member 7
439 of Olorgesailie (Isaac 1977), but slightly younger than the group of sites from Olorgesailie
440 Member 1, and Isinya.

441 3.2.2.3 *The Ash Flow Tuff*

442 The three banded tuff is usually overlain by around 15 metres of reddish tuffaceous sediments
443 (the Farmhouse Cliff Beds: Bishop 1978; Gowlett et al. 2015), capped by a brown, massive
444 non-welded lapilli-ash tuff with thickness of some seven metres. The latter is a facies of the
445 “Lower Menengai” Tuff mapped by Jones (1975) (see also Jones and Lippard 1979), and like
446 the 3BT, it is widespread in the area south of Kilombe mountain. According to Jones, to the
447 SE, closer to Menengai caldera, the tuff units are developed with a great thickness of pumice
448 which he states passes laterally into waterlain reworked tuff. Bombs within the pumice tuff
449 become larger towards Menengai, indicating an origin from that source, rather than from
450 Kilombe or Londiani volcanoes. The pumice-bearing unit is followed by the characteristic
451 massive unwelded ash flow tuff (AFT) facies which is prominent in the Kilombe area. Main
452 components are pumice clasts, compact obsidian and trachyte clasts, and feldspar crystals.
453 Jones and Lippard (1979) describe it as ‘a succession of pumiceous tuffs capped by an
454 unwelded ignimbrite’ (p. 699). As a resistant layer it has been largely responsible for the
455 preservation of the underlying softer sediments. It is breached by erosion in the area of the
456 Main Site (GqJh1), forming cliffs that face north into the Kibberenge valley. To the south it
457 can be traced continuously into the valley of the Molo river which it mantles. In sequences the
458 AFT is usually the capping horizon, but in the area of Moricho 2 km to the west of Kilombe it
459 is overlain by a succession of younger Middle Pleistocene sediments now also dated (see
460 below).

461 The AFT has been dated at two places in the zone south of the mountain, both from the
462 Farmhouse cliff which overlooks the main site (GqJh1): Kil 1-3 is 0.461 ± 0.014 Ma and Kil
463 1-4 is 0.487 ± 0.011 Ma. At the 2-sigma confidence level these ages are indistinguishable and
464 taking into accounts the uncertainties these samples define a weighted mean age for the AFT
465 of 0.474 ± 0.009 Ma.

466 These deposits have a normal magnetic polarity, confirming that the AFT formed during the
467 Brunhes Chron at <790 ka (Mark et al., 2017), consistent with the Middle Pleistocene $^{40}\text{Ar}/^{39}\text{Ar}$
468 age. Jones (1979) termed this marker “Lower Menengai” Tuff and mapped it as occurring
469 within Kilombe caldera (as noted above).

470 Also within the Menengai assemblage is a trachyte, which was ^{40}K - ^{40}Ar dated by Jones and
471 Lippard (1979) from a trachyte boulder in Menengai caldera to ca. 0.30 Ma, although they
472 commented on the unreliability this age, and the context is also unverifiable. It was placed at
473 the base of the Lower Menengai series, and was hitherto the only direct dating evidence
474 available.

475 Leat (1984) argued that the AFT visibly capping Farmhouse Cliff was of Upper Pleistocene
476 age, relating to a later eruption of Menengai thought to be at about 30 ka, and which has now
477 been $^{40}\text{Ar}/^{39}\text{Ar}$ dated to ca. 36 ka by Blegen et al. (2016). Jones (1985) regarded Leat’s
478 interpretation as a misidentification, perhaps a confusion with later Menengai ashes which
479 occur in the direction of Rongai. The stratigraphy at Moricho, the archaeology, and the new
480 sequence of $^{40}\text{Ar}/^{39}\text{Ar}$ ages combine to show definitively the Middle Pleistocene age of the
481 AFT. One or two Acheulean handaxes occur within the Farmhouse Cliff sediments as high as
482 one metre below the AFT: they would have an age of ca 0.5 Ma assuming a reasonable
483 sedimentation rate, and are the youngest expressions of the Acheulean known in the area so
484 far.

485 The new $^{40}\text{Ar}/^{39}\text{Ar}$ ages demonstrate that a major volcanic eruption, possibly on the scale of a
486 caldera-forming event took place during the Middle Pleistocene ca. 0.5 Ma. Jones (1975) on
487 the basis of mapping close to Menengai mountain interpreted this as activity of a ‘proto-
488 Menengai’, but there is also evidence of an eruption of Eburu volcano at a similar age (McCall
489 1967). In places surfaces of the AFT exposed by erosion may be overlain directly by a recent
490 tuff, the Rongai black ash, mentioned by Bishop (1978), Jones (1975) and Jones and Lippard
491 (1979).

492 3.2.2.4 *Esageri Beds*

493 Usually the AFT is present as a capping feature, as at Farmhouse Cliff, where it can be traced
494 along two or three kilometres of north-facing scarp. Further east, however, and to the west at
495 Moricho, where there were lows in the ancient topography, the tuff is overlain by suites of
496 younger sediments, mainly the Esageri Beds, the main component of Jones’s Menengai

497 assemblage (see Figure 3, stratigraphic overview). At Moricho these are exposed in spectacular
 498 cliffs of 10-20 m height (Jennings 1971). They contain Middle Stone Age artefacts, including
 499 typical Levallois points of lava and obsidian, but usually the contexts of these cannot be defined
 500 because of the steepness of the exposures. In the area GqJh 20 (Figure 2) a small low outlier
 501 of sediments allowed archaeological investigation. This area is a few metres above the AFT,
 502 although it is not locally visible, and three tuffs have been dated from the lower part of this
 503 sequence, in ascending order:

504	Kil 3-5	Unit 105	0.266 ± 0.003 Ma
505	Kil 3-4	Unit 104	0.275 ± 0.011 Ma
506	Kil 3-3	Unit 103	0.248 ± 0.004 Ma

507 The three tuffs are separated by thin layers of sediments containing MSA artefacts at the
 508 sampling point (Figure 5). The pieces include one small flake of obsidian, several flakes of
 509 lava, and a simple core on a cobble. There are no classic MSA points.

510 The finds occurred at low density in brown silty claystones which are very compacted. The
 511 tuffs are separated by ~2m vertically (Figure 5), suggesting that they reflect different volcanic
 512 events. When considering the uncertainty reported, the mean $^{40}\text{Ar}/^{39}\text{Ar}$ ages for Kil 3-3 and
 513 Kil 3-5 are indistinguishable. Together they place early Middle Stone Age evidence at ca. 250-
 514 265 ka. Similar ages are known for early MSA in the Baringo area, as well as at Ologesailie
 515 (Johnson and McBrearty 2010; McBrearty 1999; Blegen 2017; Deino et al. 2018; Brooks et al.
 516 2018).

517 3.2.2.5 GqJh3 West Area

518 The Esageri Beds were cut into by later incisional features, visible at the north end of the
 519 Moricho exposures, and also apparent in the Kilombe (GqJh1) main site area (Bishop 1978).
 520 At the locality GqJh 3 West-200 (Figure 2), about 1 km west of the main site area, and
 521 investigated from 2011, a long modern erosional ‘amphitheatre’ trending E-W exposes most
 522 of the local sequence in sections about 8 m high. Trachyphonolite is visible in places, overlain
 523 by brown claystones and then the 3 banded tuff. Above the 3BT is an unconformity (cutting
 524 out the 3BT at the eastern end of the exposures), and a succession of younger beds about 3
 525 metres thick. A thin yellow-brown tuff (Kil 2-7) in the in-fill is associated with *in situ* MSA
 526 artefacts (Figure 5) and has been $^{40}\text{Ar}/^{39}\text{Ar}$ dated to 0.127 ± 0.030 Ma.

527 The artefacts at site 200 include long MSA points of obsidian (Hoare et al. 2020). The majority
528 were found on the surface, but several obsidian flakes were recovered *in situ* just above and
529 within the tuff. The $^{40}\text{Ar}/^{39}\text{Ar}$ age indicates that the channel formation and filling took place
530 during the last interglacial *sensu lato* (MIS 5). A similar finding is supported by a further date
531 of 0.111 ± 0.020 Ma (Kil-2-1) for a pale gritty-textured tuff occurring at the top of the fill of
532 an incised feature on the main site GqJh1. It contains a few MSA artefacts in its basal layer.

533 The $^{40}\text{Ar}/^{39}\text{Ar}$ age is important for defining the continuation of Middle Stone Age human
534 activity. Together with the $^{40}\text{Ar}/^{39}\text{Ar}$ age for the AFT and the early MSA, places the
535 neighbouring Moricho exposures within a bracket of ca. 0.47 – 0.12 Ma.

536

537 **4. Discussion**

538 The $^{40}\text{Ar}/^{39}\text{Ar}$ ages and stratigraphic settings detailed here represents a significant step forward
539 in establishing a chronology for events in the central Kenyan Rift Valley, and also provides
540 chronological resolution to archaeological sites or faunal localities at various points in the
541 =stratigraphic succession. In its two main parts, the described sequence provides a new major
542 Pleistocene record.

543 The stratigraphic evidence, and the series of $^{40}\text{Ar}/^{39}\text{Ar}$ dates, coupled with the palaeomagnetic
544 record, demonstrate that a major part of the Pleistocene is represented by volcanics and
545 sediments forming Kilombe Volcano, within its caldera (>100 m), and on its flanks (>50 m).
546 The dating evidence has also established approximate chronostratigraphic relationships
547 between the two areas of sedimentation within and outside Kilombe Volcano. Archaeological
548 traces are included within this record almost throughout its length, in at least ten discrete levels.

549 **4.1 Significance of the Kilombe caldera-fill sequence**

550 Although Early Pleistocene localities with fauna and/or hominin occupation have become more
551 numerous in recent years, they remain sparse along much of the Central Rift Valley. Within
552 the Baringo Basin they include Chemeron 70 km to the north in the Kapthurin area (Deino and
553 Hill 2002; Deino et al. 2002; Sherwood et al. 2002), and the Chemoigut Formation on the
554 eastern side of Lake Baringo at Chesowanja (Bishop et al. 1975, 1978; Gowlett et al. 1981).
555 But Chemeron does not have archaeological sites, and Chesowanja is not known to date beyond
556 ~1.5 Ma. There is a gap of ca. 450 km to the north to the sites of East and West Turkana (Roche

557 et al. 1999; Delagnes and Roche 2005; Harmand et al. 2015; Lepre et al. 2011; Isaac et al.
558 1997), and of 180 km to Kanam to the SW (Braun et al 2009, 2010; Plummer and Bishop 2016;
559 Plummer et al. 1999). Olduvai Gorge lies 350 km to the south (Leakey, 1971; Leakey and Roe
560 1994; Deino 2012, Blumenschine et al. 2003, 2009, 2012a.b, Dominguez-Rodrigo et al. 2013;
561 Diez-Martin et al., 2015; Uribelarrea, D., 2017). The Kilombe caldera setting stands out from
562 all these other sequences through its high altitude – about 500 metres more elevated than any
563 other early East African archaeological locality, and perhaps even more important, it presents
564 a steep and rugged landscape for which there has not previously been evidence of early hominin
565 occupation from elsewhere in eastern Africa. The great majority of early Pleistocene hominin
566 localities are preserved adjacent to lake, wetland or stream settings, all well away from the
567 nearest major volcanic centres.

568 Biases in the representation of early sites on the landscape were made a focus of interpretation
569 by Glynn Isaac (e.g. 1986). He noted the low likelihood of upland sites being preserved. More
570 specific focuses on the issue of have come from the work of Blumenschine and Peters at
571 Olduvai, and from studies of tool transport at Kanam and Kanjera. Peters and Blumenschine
572 (1995) examined land use potential around Olduvai, and in a succession of papers (e.g.
573 Blumenschine and Peters 1998; Blumenschine et al. 2003, 2009, 2012a, 2012b) sought to
574 hypothesize and make tests of optimal and less optimal palaeoecologies and
575 palaeoenvironments (affordances) in which early tool-making hominins (such as *Homo habilis*)
576 would have exploited areas of the African Rift System and associated volcanic highlands,
577 considering also their possible seasonal basis (Blumenschine and Peters 1998). The Olduvai
578 area was used as a test case, and it was deduced that optimal conditions would have been river-
579 flanked areas high in the volcanic highlands, with access to fruits and rootstocks of those
580 forested areas, as well as carcasses for scavenging. By contrast, settings more typically
581 preserved geologically, and subsequently excavated archaeologically, tended to be at lower
582 levels, where affordances for hominin survival were more ephemeral and marginal. At that
583 time it was considered that environmental settings high on the volcano and its flanks were
584 unlikely candidates for preservation.

585 The caldera setting at Kilombe however shows how a lacustrine sequence with fluvial and fan
586 sequences prograding into the lake can be preserved high on a volcano. A good modern
587 analogue is Ngorongoro Caldera, which formed, probably through major eruption and
588 subsequent subsidence (Hay, 1976) ~2 Ma ago, and which still contains saline-alkaline Lake

589 Makat with surrounding freshwater wetlands. Fan sedimentation proceeds off the caldera rim
590 and fluvial input via the River Munge, providing analogue lateral settings where in the past
591 hominins might have thrived.

592 Thus the occurrences discovered in the fill-sequence of Kilombe Caldera present an
593 extremely rare opportunity to explore sites exploited by early hominins that were set in
594 highlands, and potentially to contrast their archaeological characteristics with those in better-
595 known lowland settings such as FLK Level 22 (Leakey, 1971; Blumenschine et al., 2012a;
596 Dominguez-Rodrigo et al. 2007) and HWK E Level 1 (Leakey, 1971; Blumenschine et al.,
597 2012b).

598 As of now artefacts are known from at least two stratigraphic zones in the caldera. The
599 lower, dating to ~1.8 Ma appears to have Oldowan characteristics in a generic sense. The
600 presence in low numbers of choppers and flakes is entirely compatible with an Oldowan
601 designation (currently locality GqJh13A has produced ~30 heavy-duty forms, and ~50 flakes
602 and other debitage: Gowlett et al. in prep). Locally sourced trachyte appears to be the
603 dominant raw material. It does not usually give high quality conchoidal fracture, but was
604 adequate for providing robust sharp edges. Acheulean artefacts in some numbers come from
605 a zone about 30 metres higher in the sequence. They have been found *in situ* both on the
606 surface embedded in sediment, and in step trenches. About 30 specimens have been found,
607 including six bifaces or biface flakes. The date of the finds at the top of the upper staircase is
608 not yet closely fixed, although they are younger than ~1.76 Ma. Like the Oldowan finds,
609 they are made almost entirely of trachyte, without signs of the trachyphonolite that was
610 widely used for bifaces outside the caldera, and which was deposited at ~1.56 Ma (see
611 below). The specimens within the caldera could well be older than this date, but further work
612 is necessary to clarify this issue.

613 **4.2. Significance of the Kilombe mountain flank sequence**

614 The southern mountain flank sequence includes Acheulean sites which have been known since
615 the 1970s, but the new work greatly extends the sequence and improves its chronology. The
616 dates for the trachyphonolite lava establish a base of ca 1.57 Ma for the main Kilombe sequence
617 on the flanks of the mountain – shared approximately with basal dates for the Kapthurin
618 Formation at Baringo, Kenya (Deino and McBrearty 2002). As the earliest dates obtained for
619 the Acheulean in East Africa are older than this (e.g. West Turkana, Konso Gardula, and

620 Olduvai (LePre et al. 2011; Beyene et al. 2013, 2015; de la Torre 2016; Diez-Martín et al. 2015),
621 an Acheulean presence would be possible even down to the base of the southern flank sequence
622 in the Kilombe area, but outside the caldera no Acheulean traces have yet been found at levels
623 lower than the main site (GqJh1, Figures 2, 5.), now well dated to ~1.0. Ma.

624 The extensive Acheulean of the Main Site (GqJh1) thus remains the oldest at Kilombe outside
625 the caldera. Its date of around 1.0 Ma is very close to that for Kariandusi, 80 km to the SE
626 (Durkee and Brown 2014; Gowlett 1980; Gowlett and Crompton 1994). Dates at Kariandusi
627 appear to be slightly under one million years for the Upper Site localities containing many
628 obsidian handaxes, and certainly $>\sim 800,000$ on the basis of the palaeomagnetic evidence. In a
629 tuff correlation study Durkee and Brown (2014) confirmed a similar date for Isinya, while the
630 oldest dates for the Olorgesailie Formation, just above the artefact horizons of Member 1, are
631 also around 0.974 -0.992 Ma (Durkee and Brown 2014; Isaac 1977; Potts et al. 1999). These
632 dates coincide with a long wet phase in the Rift Valle noted by Trauth et al. (2005).

633 The central Rift Valley region in Kenya provides very rare opportunities for comparing
634 *penecontemporaneous* Acheulean assemblages (cf Isaac 1977; Gowlett 2015). At Kilombe
635 itself, the stratigraphic range of the Acheulean established so far is from the main horizon below
636 the 3BT up to a point immediately below the AFT – covering a period of about 0.5 million
637 years. Metrical and morphological comparisons are possible between the main horizon and
638 two sets of bifaces from the Farmhouse Cliff sediments: around 20 bifaces from Kilombe
639 GqJh3 West (KW) come from layers up to 5 m above the three banded tuff, and so somewhat
640 lower than another set from the northeastern gullies (Figure 2, Kilombe GqJh2 South NE).
641 These last correlate with higher levels of the Farmhouse Cliff sediments, close to the position
642 of the Brunhes-Matuyama boundary. The comparisons of bifaces made so far suggest that the
643 basic pattern of Kilombe bifaces generally made of trachyphonolite, and having a mean length
644 of ca. 150 mm, was maintained between 1 million years and the B/M boundary 200 ka later
645 without obvious change (Gowlett 2015). A similar pattern may be maintained because of the
646 use of the same raw materials, perhaps encouraging a similar mean size of the large flakes used
647 as bifaces blanks (cf Sharon 2007).

648 The AFT has importance as a stratigraphic marker, and also potentially has great use
649 chronostratigraphically as its time point of ca 0.5 Ma is often difficult to date at high resolution
650 in archaeological sequences except when $^{40}\text{Ar}/^{39}\text{Ar}$ geochronology can be applied. Boxgrove
651 in Britain is one of the few sites that can be pinned to this period outside Africa (Roberts and

652 Parfitt 1999; Pope and Roberts 2005). There is, however, widespread interest in the dating of
653 technological changes which may begin from around this time in Africa, and which culminate
654 eventually in expressions of the MSA (e.g. Barham 2013; Basell 2008; Blome et al. 2012;
655 Brooks et al. 2018; McBrearty and Brooks 2000; Pleurdeau 2006; Wendorf and Schild 1974).
656 Johnson and McBrearty (2010) highlight the early presence of stone blades at Kapthurin at this
657 time, and according to Wilkins et al. (2012), major technological change can also be detected
658 from this period at Kathu Pan in southern Africa, where projectile points suitable for hafting
659 were dated by use of OSL on sediments. On the Kilombe southern flanks the Acheulean occurs
660 very sporadically in the upper part of the levels between the Main Site (GqJh1) and the AFT.
661 One handaxe was found just one metre below the tuff, just north of GqJh2. Also in GqJh2 area,
662 a double-pointed biface was found, close to the AFT level. This distinctive form is reminiscent
663 of later Lupemban forms, and can also be matched by one example from Olorgesailie (Isaac
664 1977, Figure 73, p.221). Until now no handaxes have been found above the AFT, although
665 the lower levels at Moricho at ~280 ka are demonstrably within a time-range where both
666 Middle Stone Age and late Acheulean facies might be found (cf finds under the ca. 280ka
667 capping tuff at Kapthurin: McBrearty 1999; Tryon 2006; Tryon and McBrearty 2002, 2006;
668 Deino et al. 2018).

669 The upper sequence around Kilombe is complex. There was further sedimentation above the
670 AFT, especially in depressions, as at Moricho to the west of Kilombe, and to the east of the
671 trachyphonolite spur where the small Kibberenge valley descends parallel to the River Molo
672 (Figure 2). These are the thick red beds noted by Jennings (1971) and named by Jones (1975)
673 as the Esageri Beds. Channels, sometimes containing tuffs in their fill, cut into the upper levels
674 of these beds, both at Moricho and at Kilombe. The most important locality to date occurs
675 about halfway between Moricho and Kilombe, two kilometres west of the Kilombe Main Site
676 (GqJh1). This is the Middle Stone Age locality of Kilombe GqJh3 West 200, now dated to 127
677 ± 30 ka at 1σ (Hoare et al. 2020); the date of 111 ± 20 ka from the main site GqJh1 confirms
678 sedimentary cycle and human presence at about the same time. Geochemical analysis
679 undertaken on Obsidian points from this locality suggests the use of multiple sources and the
680 long-distance transportation of high-quality obsidian from over 80 km away in MIS 5. The
681 outline sequence of Middle Stone age localities presented here is now relatively well-dated,
682 but more work will be needed to elaborate it archaeologically. Artefacts, mainly of obsidian,
683 occur at low density in the known localities. Where there are denser obsidian scatters they tend
684 to have accumulated at the base of steep cliffs, making further exploration challenging. There

685 are however places where overlying levels have been eroded away, and the relevant localities
686 are more accessible. The finds already add to the regional picture of a MSA deeply established
687 in time (Basell 2008), probably from around 300 ka, and with transport of obsidian materials
688 from distant sources, as established by Blegen et al. 2016 at Baringo.

689

690 5. Conclusion

691 The new investigations across Kilombe Volcano, on its flanks and within its caldera, coupled
692 with the palaeomagnetic evidence and a series of new $^{40}\text{Ar}/^{39}\text{Ar}$ dates, demonstrate a major
693 new sequence of lava flows and tuffs, fluvio-lacustrine sediments and archaeology ranging
694 through almost the entire Pleistocene. It is one of the more complete of such sequences, and
695 the only one which was generated in a highland context, significantly demonstrating early
696 hominin presence at highpoints in the rugged landscape. The dates confirm that the major
697 feature of the landscape, Kilombe Volcano itself, assumed something like its present shape
698 ~2.5Ma years ago. Bedded tuffs and lake sediments accumulated within its caldera and
699 evidently, at times between eruptions, the area surrounding an intra-caldera lake presented an
700 attractive environment to animals. These included large mammals such as hippopotamus (the
701 extinct *Hippopotamus gorgops*) found in new faunal localities of an age corresponding to
702 Olduvai Bed I. The presence of early artefacts at multiple localities proves for the first time
703 that early hominins regularly exploited these topographically upland settings.

704 The lack of trachyphonolite artefacts within the caldera might indicate that Acheulean artefacts
705 there are likely to be older than those known outside the mountain, but further research is
706 required to validate this point.

707 The Acheulean occurrences on the lower flanks of the mountain are now documented to occur
708 through most of the time range 1.0 – 0.5 Ma. The oldest remain those of the Main Site (GqJh1),
709 about one metre below the approximately million-year-old Three-banded Tuff (3BT); the
710 youngest, immediately below the Ash Flow Tuff (AFT), is around half that age. The AFT
711 represents a cataclysmic eruption in the area, probably from the Menengai direction, and it,
712 together with its underlying unconformity surface provides a benchmark for
713 chronostratigraphic studies in the region. Further work will be needed to determine a full
714 chronology for the later Middle to Upper Pleistocene deposits of Moricho and Kilombe
715 overlying the AFT, but key points are already established, through the dates for early MSA

716 sites in the range ~ 250-270 ka at Moricho (Figures 2, 3), and in the date for the Middle Stone
717 Age MSA site GqJh3W-200, which belongs to the beginning of the Upper Pleistocene,
718 approximately 120,000 years ago. Later Stone Age surface sites complete the sequence.

719 Above all, the Kilombe sedimentary archive records the repeated presence of early humans in
720 the one area. The evidence from Kilombe mountain includes traces of well-watered
721 environments at several times in the past, with hippopotamus featuring in at least three levels.
722 Early and later hominins may have exploited these environments in the repeated way that we
723 observe partly because of the ecotonal aspect that a variety of resources were available within
724 a few kilometres at very different altitudes. The Kilombe record therefore now provides
725 exceptional opportunities for further research on landscape and its use by hominins through the
726 extent of the Pleistocene.

727

728 **Acknowledgments**

729 Funding: fieldwork support has been received from The Leverhulme Trust grant [RPG-2017-
730 183], PAST Foundation, Wenner-Gren Foundation [Gr. 9536], and a British Academy-
731 supported Mobility and Links Project between University of Liverpool and National Museums
732 of Kenya (2013-2016). The dating work was supported by NERC awards IP-354-1112 and
733 IP-1617-0516. NERC are thanked for continued support of the $^{40}\text{Ar}/^{39}\text{Ar}$ facility at SUERC.
734 JAJG is grateful for support from the British Academy Centenary Project, and help and
735 permissions from NACOSTI and National Museums of Kenya. SH is grateful for support from
736 the AHRC (PhD studentship) and NERC and SUERC. AH acknowledges funding from the
737 Australian Research Council via Future Fellowship FT 120100399. Thanks are owed to Willy
738 Jones, Laura Basell, Fabienne Marret-Davies, Darren Curnoe, Robin Crompton, Stephen
739 Lycett, Ginette Warr, Sian Davies, Mimi Hill and Natalie Uomini; to the Commissioner for
740 Baringo County, Mr H. Wafula; and our Kenyan helpers at Kilombe Caldera, especially Mr
741 Philip Kogai. We also thank Maura Butler; and those who are still missed: Jean-Claude (J.C.)
742 Tubiana, Bill Bishop, and our colleague and co-author James Brink.

743

744 **References**

745 Barham, L., 2013. *From hand to handle: the first industrial revolution*. Oxford University
746 Press, Oxford.

- 747 Basell, L.S., 2008. Middle Stone Age (MSA) site distributions in eastern Africa and their
748 relationship to Quaternary environmental change, refugia and the evolution of Homo
749 sapiens. *Quaternary Science Reviews* 27, 2484-2498.
- 750 Beyene, Y., Katoh, S., WoldeGabriel, G., Hart, W.K., Uto, K., Kondo, M., Hyodo, M.,
751 Renne, P.R., Suwa, G., Asfaw, B., 2013. The characteristics and chronology of the
752 earliest Acheulean at Konso, Ethiopia. *Proc. Natl Acad. Sci. USA* 110, 1584–1591.
753 <https://doi/10.1073/pnas.1221285110>.
- 754 Beyene, Y., Asfaw, B., Sano, K., Suwa, G., 2015. Konso-Gardula Research Project Volume 2:
755 Archaeological collections: Background and the Early Acheulean assemblages.
756 Bulletin 48, the University Museum, the University of Tokyo, Tokyo.
- 757 Bishop, W.W., 1978. Geological framework of the Kilombe Acheulian Site, Kenya, in:
758 Bishop, W.W. (Ed.), *Geological Background to Fossil Man*. Scottish Academic Press,
759 Edinburgh, pp. 329-336.
- 760 Bishop, W.W., Hill, A., Pickford, M., 1978. Chesowanja: a revised geological
761 interpretation, in Bishop, W.W. (Ed.), *Geological background to fossil man*. Scottish
762 Academic Press, Edinburgh, pp. 309-328.
- 763 Bishop, W.W., Pickford, M., Hill, A., 1975. New evidence regarding the Quaternary
764 geology, archaeology, and hominids of Chesowanja, Kenya. *Nature* 258, 204-208.
- 765 Blegen, N., 2017. The earliest long-distance obsidian transport: evidence from the ~200 ka
766 Middle Stone Age Sibilo School Road site, Baringo, Kenya. *Journal of Human
767 Evolution* 103, 1-19.
- 768 Blegen, N., Brown, F.H., Jicha, B.R., Binetti, K.M., Faith, J.T., Ferraro, J.V., Gathogo, P.N.,
769 Richardson, J.L., Tryon, C.A., 2016. The Menengai Tuff: a 36 ka widespread tephra
770 and its chronological relevance to Late Pleistocene human evolution in East Africa.
771 *Quaternary Science Reviews* 152, 152e168.
- 772 Blome, M.W., Cohen, A.S., Tryon, C.A., Brooks, A.S., Russell, J., 2012. The environmental
773 context for the origins of modern human diversity: A synthesis of regional variability
774 in African climate 150,000–30,000 years ago. *Journal of Human Evolution* 62, 563-
775 592.
- 776 Blumenschine, R.J., Peters, C.R., 1998. Archaeological predictions for hominid land use in
777 the paleo-Olduvai Basin, Tanzania, during lowermost Bed II times. *Journal of Human
778 Evolution* 34, 565-607.
- 779 Blumenschine, R.J., Peters, C.R., Masao, F.T., Clarke, R.J., Deino, A.L., Hay, R.L., Swisher,
780 C.C., Stanistreet, I.G., Ashley, G.M., McHenry, L.J., Sikes, N.E., van der Merwe, N.J.,
781 Tactikos, J.C., Cushing, A.E., Deocampo, D.M., Njau, J.K., Ebert, J.I., 2003. Late
782 Pliocene Homo and hominid land use from western Olduvai Gorge, Tanzania. *Science*
783 299, 1217-1221
- 784 Blumenschine, R., Masao, F.T., Stanistreet, I.G., 2009. Changes in hominin transport of stone
785 tools across the eastern Olduvai Basin during lowermost Bed II times, in: Schick, K.,
786 Toth, N. (Eds.), *The Cutting Edge: New Approaches to the Archaeology of Human
787 Origins*. Stone Age Institute Press, Gosport, pp. 1-15.
- 788 Blumenschine, R.J., Stanistreet, I.G., Njau, J.K., Bamford, M.K., Masao, F.T., Albert, R.M.,
789 Stollhofen, H., Andrews, P., Prassack, K.A., McHenry, L.J., Fernandez-Jalvo, Y.,
790 Camilli, E.L., Ebert, J.I., 2012a. Environments and activity traces of hominins across
791 the FLK Peninsula during Zinjanthropus times (1.84 Ma), Olduvai Gorge, Tanzania,

- 792 in: Blumenschine, R.J., Masao, F.T., Stanistreet, I.G., Swisher, C.C. (Eds.), Five
793 Decades after Zinjanthropus and Homo habilis: Landscape Paleoanthropology of Plio-
794 Pleistocene Olduvai Gorge, Tanzania. *Journal of Human Evolution* 63(2), 364e383.
- 795 Blumenschine, R.J., Masao, F.T., Stollhofen, H., Stanistreet, I.G., Bamford, M.K., Albert,
796 R.M., Njau, J.K., Prassack, K.A., 2012b. Landscape distribution of Oldowan stone
797 artifact assemblages across the fault compartments of the eastern Olduvai Lake Basin
798 during early lowermost Bed II times, in: Blumenschine, R.J., Masao, F.T., Stanistreet,
799 I.G., Swisher, C.C. (Eds.), Five Decades after Zinjanthropus and Homo habilis:
800 Landscape Paleoanthropology of Plio-Pleistocene Olduvai Gorge, Tanzania. *Journal of*
801 *Human Evolution* 63(2), 384e394.
- 802 Braun, D., Plummer, T. W., Ferraro, J., Ditchfield, P., Bishop L., 2009. Raw material quality
803 and Oldowan hominin toolstone preferences: Evidence from Kanjera South. *Journal*
804 *of Archaeological Science* 36, 1605–1614.
- 805 Braun, D.R., Harris, J.W.K., Levin, N.E., McCoy, J.T., Herries, A.I.R., Bamford, M.K.,
806 Bishop, L.C., Richmond, B.G., Kibunjia, M., 2010. Early hominin diet included
807 diverse terrestrial and aquatic animals 1.95Ma in East Turkana, Kenya. *Proc. Natl.*
808 *Acad. Sci. USA* 107, 10002-10007.
- 809 Brooks, A.S., Yellen, J.E., Potts, R., Behrensmeyer, A.K., Deino, A.L., Leslie, D.E.,
810 Ambrose, S.H., Ferguson, J.R., d’Errico, F., Zipkin, A.M., Whittaker, S., Post, J.,
811 Veatch, E.G., Foecke, K., Clark, J.B., 2018. Long-distance stone transport and
812 pigment use in the earliest Middle Stone Age. *Science* 360, 90-94.
813 <https://doi/10.1126/science.aao2646>.
- 814 Dagley, P., Mussett, A.E., Palmer, H.C., 1978. Preliminary observations on the
815 palaeomagnetic stratigraphy of the area west of Lake Baringo, Kenya, in: Bishop,
816 W.W. (Ed.), *Geological Background to Fossil Man*. Scottish Academic Press,
817 Edinburgh, pp. 225-236.
- 818 Deino, A.L. 2012. $^{40}\text{Ar}/^{39}\text{Ar}$ dating of Bed I, Olduvai Gorge, Tanzania, and the chronology of
819 early Pleistocene climate change. *Journal of Human Evolution* 63, 251-73.
820 <https://doi/10.1016/j.jhevol.2012.05.004>.
- 821 Deino, A.L., Hill, A., 2002. $^{40}\text{Ar}/^{39}\text{Ar}$ dating of the Chemeron Formation strata encompassing
822 the site of hominid KNM-BC 1, Tugen Hills, Kenya. *Journal of Human Evolution* 42,
823 141-151.
- 824 Deino, A.L., McBrearty, S. 2002. $^{40}\text{Ar}/^{39}\text{Ar}$ dating of the Kapthurin Formation, Baringo, Kenya
825 *Journal of Human Evolution* 42, 185–210. <https://doi/10.1006/jhev.2001.0517>.
- 826 Deino, A.L., Tauxe, L., Monaghan, M., Hill, A., 2002. $^{40}\text{Ar}/^{39}\text{Ar}$ geochronology and
827 paleomagnetic stratigraphy of the Lukeino and lower Chemeron succession at Tabarin
828 and Kapcheberek, Tugen Hills, Kenya. *Journal of Human Evolution* 42, 117-140.
- 829 Deino, A.L., Behrensmeyer, A.K., Brooks, A.S., Yellen, J.E., Sharp, W.D., Potts, R., 2018.
830 Chronology of the Acheulean to Middle Stone Age transition in eastern Africa.
831 *Science*, eaao2216. <https://doi/10.1126/science.aao2216>.
- 832 Delagnes, A., Roche, H., 2005. Late Pliocene hominid knapping skills: the case of Lokalalei
833 2C, West Turkana, Kenya. *Journal of Human Evolution* 48, 435-472.
- 834 Diez-Martín, F., Yustos, P.S., Uribelarrea, D., Baquedano, E., Mark, D.F., Mabulla, A.,
835 Fraile, C., Duque, J., Díaz, I., Pérez-González, A., Yravedra, J., 2015. The origin of

- 836 the Acheulean: the 1.7 million-year-old site of FLK West, Olduvai Gorge (Tanzania).
837 *Scientific Reports*, 5. Dec 7. <https://doi/10.1038/srep17839>
- 838 Domínguez-Rodrigo M., Barba R., Egeland C., 2007. *Deconstructing Olduvai: a taphonomic*
839 *study of the Bed I sites*. Springer, Dordrecht.
- 840 Domínguez-Rodrigo, M., Pickering, T.R., Baquedano, E., Mabulla, A., Mark, D.F., Musiba,
841 C., Bunn, H.T., UribeArrea, D., Smith, V., Diez-Martin, F., Pérez-González, A.,
842 Sánchez, P., Santonjaa, M., Barboni, D., Gidna, A., Ashley, G., Yravedra, J., Heaton,
843 J.L., Arriaza, M.C., 2013. First partial skeleton of a 1.34-million-year-old
844 *Paranthropus boisei* from Bed II, Olduvai Gorge, Tanzania. *PLoS ONE* 8, e80347.
- 845 Durkee H., Brown F.H., 2014. Correlation of volcanic ash layers between the Early
846 Pleistocene Acheulean sites of Isinya, Kariandusi, and Olorgesailie, Kenya. *Journal of*
847 *Archaeological Science* 49, 510-517.
- 848 Gowlett, J.A.J., 1978. Kilombe - an Acheulean site complex in Kenya, in: Bishop, W.W. (Ed.),
849 *Geological Background to Fossil Man*. Scottish Academic Press, Edinburgh, pp. 337-
850 360.
- 851 Gowlett, J.A.J. 1980. Acheulean sites in the Central Rift Valley, Kenya, in: Leakey, R.E.,
852 Ogot, B.A. (Eds.) *Proceedings of the 8th Panafrican Congress of Prehistory and*
853 *Quaternary Studies, Nairobi, 1977*. TILMIAP, Nairobi, pp. 213-217.
- 854 Gowlett, J.A.J., 1993. Le site Acheuléen de Kilombe: stratigraphie, géochronologie, habitat et
855 industrie lithique. *L'Anthropologie* 97 (1), 69-84.
- 856 Gowlett, J.A.J., 2015. Variability in an early hominin percussive tradition: the Acheulean
857 versus cultural variation in modern chimpanzee artefacts. *Phil. Trans. R. Soc. B* 370,
858 20140358. <https://doi/10.1098/rstb.2014.0358>.
- 859 Gowlett, J.A.J., Crompton, R. H., 1994. Kariandusi: Acheulean morphology and the question
860 of allometry. *The African Archaeological Review* 12:3-42.
- 861 Gowlett, J.A.J., Brink, J.S., Herries, A.I.R., Hoare, S., Rucina, S.M., 2017. The small and
862 short of it: mini-bifaces and points from Kilombe, Kenya, and their place in the
863 Acheulean, in: Wojtczak, D., Al Najjar, M., Jagher, R., Elsuede, H., Wegmüller, F.
864 (Eds) *Vocation Préhistoire: Homage à Jean-Marie Le Tensorer*. ERAUL 148, Liège,
865 pp. 121-132.
- 866 Gowlett, J.A.J., Brink, J.S., Herries, A.I.R., Hoare, S., Onjala, I, Rucina, S.M., 2015. At the
867 heart of the African Acheulean: the physical, social and cognitive landscapes of
868 Kilombe, in: Coward, F., Hosfield, R., Wenban-Smith, F. (Eds.), *Settlement, Society*
869 *and Cognition in human evolution: Landscapes in Mind*. Cambridge University
870 Press, Cambridge, pp. 75-93.
- 871 Gowlett, J.A.J., Harris, J.W.K., Walton, D. and Wood, B.A. 1981. Early archaeological sites,
872 hominid remains and traces of fire from Chesowanja, Kenya. *Nature* 294, 125-129.
- 873 Griffiths, P.S., Gibson, I.L., 1980. The geology and petrology of the Hannington
874 Trachyphonolite formation, Kenya Rift Valley. *Lithos* 13,43-53.
- 875 Harmand, S., Lewis, J.E., Feibel, C.S., Lepre, C.J., Prat, S., Lenoble, A., Boës, A., Quinn,
876 R.L., Brenet, M., Arroyo, A. *et al.*, 2015. 3.3-million-year-old stone tools from
877 Lomekwi 3, West Turkana, Kenya. *Nature* 521, 310-315.
- 878 Hay R.L. 1976. *Geology of the Olduvai Gorge*. University of California Press, Berkeley.

- 879 Herries, A.I.R., Davies, S., Brink, J., Curnoe, D., Warr, G., Hill, M., Rucina, S., Onjala, I.,
880 Gowlett, J.A.J., 2011. New explorations and magnetobiostratigraphical analysis of the
881 Kilombe Acheulian localitiy, Central Rift, Kenya. *Paleoanthropology* 2011, A16.
- 882 Hoare, S., Rucina, S., Gowlett, J.A.J. 2020. Initial source evaluation of archaeological obsidian
883 from Middle Stone Age site GqJh3 West 200, in: Cole, J., McNabb, J., Grove, M.,
884 Hosfield, R. (Eds.), *Landscapes of human evolution: contributions in honour of John*
885 *Gowlett*. Archaeopress, Oxford, pp. 142-149.
- 886 Isaac, G.Ll., 1977. *Olorgesailie: Archaeological Studies of a Middle Pleistocene Lake Basin*
887 *in Kenya*. University of Chicago Press, Chicago.
- 888 Isaac, G. Ll. 1986. Foundation stones: early artefacts as indicators of activities and abilities,
889 in: Bailey, G.N., Callow, P. (Eds.), *Stone Age prehistory: studies in memory of*
890 *Charles McBurney*. Cambridge University Press, Cambridge, pp. 221-241.
- 891 Isaac, G.Ll., Harris, J.W.K., Kroll, E.M., 1997. The stone artefact assemblages: a comparative
892 study, in: Isaac, G.Ll., Isaac, B. (Eds.), *Koobi Fora Research project Volume 5: Plio-*
893 *Pleistocene Archaeology*. Clarendon Press, Oxford, pp. 262-362.
- 894 Jennings, D.J., 1971. Geology of the Molo area. Ministry of Natural Resources, Geological
895 Survey of Kenya, Report No. 86.
- 896 Johnson, S.R., McBrearty, S. 2010. 500,000 year-old blades from the Kapthurin Formation,
897 Kenya. *Journal of Human Evolution* 58,193–200.
- 898 Jones, W.B., 1975. *The geology of the Londiani area of the Kenya Rift Valley*. Unpublished
899 PhD thesis, Univ. London.
- 900 Jones, W.B., 1985. Discussion on the geological evolution of the trachyte caldera volcano
901 Menengai, Kenya Rift Valley. *Journal of the Geological Society, London* 142, 711-
902 712.
- 903 Jones, W.B., 1988. Listric growth faults in the Kenya Rift Valley. *Journal of Structural*
904 *Geology* 10, 661-672.
- 905 Jones, W.B., Lippard, S.J., 1979. New age determinations and geology of the Kenya Rift-
906 Kavirondo Rift junction, W. Kenya. *Journal of the Geological Society, London* 136,
907 693-704.
- 908 Kuiper, K.F., Deino, A., Hilgen, F.J., Krijgsman, W., Renne, P.R., Wijbrans, J.R., 2008.
909 Synchronizing rock clocks of Earth history. *Science* 320 (5875), 500e504.
- 910 Leakey, M.D., 1975. Cultural patterns in the Olduvai sequence, in: Butzer, K.W., Isaac, G. Ll.
911 (Eds.), *After the Australopithecines*. Mouton, The Hague, pp. 477-494.
- 912 Leakey, M.D., Roe, D.A. (Eds.), 1994. *Olduvai Gorge, Vol. 5: Excavations in Beds III, IV*
913 *and the Masek Beds 1968-1971*. Cambridge University Press, Cambridge.
- 914 Leat, P.T., 1984. Geological evolution of the trachyte caldera volcano Menengai, Kenya Rift
915 Valley. *Journal of the Geological Society, London* 141, 1057-69.
- 916 Lee, J.Y., Marti, K., Severinghaus, J.P., Kawamura, K., Yoo, H.S., Lee, J.B., Kim, J.S., 2006.
917 A redetermination of the isotopic abundances of atmospheric Ar. *Geochimica et*
918 *Cosmochimica Acta* 70 (17), 4507e4512.
- 919 Lepre, C. J., Roche, H., Kent, D.V., Harnand, S., Quinn, R.L., Brugal, J.-P., Texier, P.-J, Feibel,
920 C.S., 2011 An earlier origin for the Acheulian. *Nature* 477, 82–85.
921 <https://doi/10.1038/nature10372>.

- 922 McBrearty, S., 1999. The Archaeology of the Kapthurin formation, in: Andrews, P., Banham,
923 P. (Eds.), *Late Cenozoic environments and hominid Evolution: a tribute to Bill Bishop*.
924 Geological Society, London, pp. 143-156.
- 925 McBrearty, S., Brooks, A.S., 2000. The revolution that wasn't: a new interpretation of the origin
926 of modern human behavior. *Journal of Human Evolution* 39, 453-563.
- 927 McCall, G.J.H., 1964. Kilombe caldera, Kenya. *Proceedings of the Geologists' Association*
928 75, 563-572.
- 929 McCall, G.J.H., 1967. *Geology of the Nakuru-Thomson's Falls-Lake Hannington area*.
930 Ministry of Natural Resources, Geological Survey of Kenya, Report No. 78
- 931 Mark, D.F., Gonzalez, S., Huddart, D., Böhnell, H., 2010. Dating of the Valsequillo volcanic
932 deposits: resolution of an ongoing archaeological controversy in Central Mexico.
933 *Journal of Human Evolution* 58 (5), 441e445.
- 934 Mark, D.F., Stuart, F.M., de Podesta, M., 2011. New high-precision measurements of the
935 isotopic composition of atmospheric argon. *Geochimica et Cosmochimica Acta* 75
936 (23), 7494e7501.
- 937 Mark, D.F., Petraglia, M., Smith, V.C., Morgan, L.E., Barfod, D.N., Ellis, B.S., Pearce, N.J.,
938 Pal, J.N., Korisettar, R., 2014. A high-precision $^{40}\text{Ar}/^{39}\text{Ar}$ age for the Young Toba
939 Tuff and dating of ultra-distal tephra: forcing of Quaternary climate and implications
940 for hominin occupation of India. *Quaternary Geochronology* 21, 90e103.
- 941 Mark, D.F., Renne, P.R., Dymock, R., Smith, V.C., Simon, J.I., Morgan, L.E., Staff, R.A., Ellis,
942 B.S., Pearce, N.J.G., 2017. High precision $^{40}\text{Ar}/^{39}\text{Ar}$ dating of Pleistocene tuffs and
943 temporal anchoring of the Matuyama-Brunhes boundary. *Quaternary*
944 *Geochronology* 39, 1-23.
- 945 Mehlman, M., 1991. Context for the emergence of Modern man in eastern Africa: some new
946 Tanzanian evidence, in: Clark, J.D. (Ed.) *Approaches to Understanding Early Hominid*
947 *life-ways in the African Savanna*. Römisch - Germanisches Zentralmuseum
948 Forschungsinstitut für Vor- und Frühgeschichte in Verbindung mit der UISSP, 11
949 Kongress, Mainz 1987. Monographien Band 19, Dr Rudolf Habelt GMBH, Bonn, pp.
950 177-196.
- 951 Merrick, H.V., Brown, F.H., 1984. Obsidian sources and patterns of source utilization in
952 Kenya and northern Tanzania: some initial findings. *African Archaeological Review* 2,
953 129-152.
- 954 Morgan, L.E., Renne, P.R., Kieffer, G., Piperno, M., Gallotti, R., Raynal, J.-P., 2012. A
955 chronological framework for a long and persistent archaeological record: Melka
956 Kunture, Ethiopia. *Journal of Human Evolution* 62,104-115.
957 <https://doi/10.1016/j.jhevol.2011.10.007>.
- 958 Niespolo, E.M., Rutte, D., Deino, A.L., Renne, P.R., 2017. Intercalibration and Age of the
959 Alder Creek Sanidine $^{40}\text{Ar}/^{39}\text{Ar}$ Standard. *Quaternary Geochronology* 39, 205-213.
- 960 Peters, C. R., Blumenshine, R. J., 1995. Landscape perspectives on possible land use
961 patterns for early hominids in the Olduvai Basin. *Journal of Human Evolution* 29,
962 321-362.
- 963 Pleurdeau, D., 2006. Human technical behavior in the African Middle Stone Age: the lithic
964 assemblage of Porc-Epic Cave (Dire Dawa, Ethiopia) *African Archaeological Review*
965 22, 177-197.

- 966 Plummer, T.W., Bishop, L.C., 2016. Oldowan hominin behaviour at Kanjera South, Kenya.
967 *Journal of Anthropological Sciences* 94, 29-40.
- 968 Plummer, T., Bishop, L.C., Ditchfield, P., Hicks, J., 1999. Research on Late Pliocene Oldowan
969 sites at Kanjera South, Kenya. *Journal of Human Evolution* 36: 151-170.
- 970 Pope, M.I., Roberts, M.B., 2005. Observations on the relationship between Palaeolithic
971 individuals and artefact scatters at the Middle Pleistocene site of Boxgrove, UK., in:
972 Gamble, C.S., Porr, M. (Eds.), *The hominid individual in context: Archaeological*
973 *investigations of Lower and Middle Palaeolithic, landscapes, locales and artefacts.*
974 Routledge, London, pp. 81-97.
- 975 Potts, R., Behrensmeyer, A.K., Ditchfield, P. 1999. Paleolandscape variation and Early
976 Pleistocene hominid activities: Members 1 and 7, Olorgesailie Formation, Kenya.
977 *Journal of Human Evolution* 37, 747-788.
- 978 Renne, P.R., 2014. Some footnotes to the optimization-based calibration of the $^{40}\text{Ar}/^{39}\text{Ar}$
979 system. Geological Society of London Special Publication 378, 21e31.
- 980 Renne, P.R., Cassata, W.S., Morgan, L.E., 2009. The isotopic composition of atmospheric
981 argon and $^{40}\text{Ar}/^{39}\text{Ar}$ geochronology: time for a change? *Quaternary Geochronology* 4
982 (4), 288e298
- 983 Renne, P.R., Norman, E.B., 2001. Determination of the half-life of ^{37}Ar by mass
984 spectrometry. *Phys. Rev. C* 63 (4), 047302.
- 985 Renne, P.R., Mundil, R., Balco, G., Min, K., Ludwig, K.R., 2011. Response to the comment
986 by W. H. Schwarz et al. on “Joint determination of ^{40}K decay constants and $^{40}\text{Ar}^*/^{40}\text{K}$
987 for the Fish Canyon sanidine standard, and improved accuracy for $^{40}\text{Ar}/^{39}\text{Ar}$
988 geochronology”. *Geochimica et Cosmochimica Acta* 75, 5097e5100.
- 989 Renne, P.R., Mundil, R., Balco, G., Min, K., Ludwig, K.R., 2010. Joint determination of ^{40}K
990 decay constants and $^{40}\text{Ar}^*/^{40}\text{K}$ for the Fish Canyon sanidine standard, and improved
991 accuracy for $^{40}\text{Ar}/^{39}\text{Ar}$ geochronology. *Geochimica et Cosmochimica Acta* 74 (18),
992 5349e5367.
- 993 Renne, P.R., Sharp, Z.D., Heizler, M.T., 2008. Cl-derived argon isotope production in the
994 CLICIT facility of OSTR reactor and the effects of the Cl-correction in $^{40}\text{Ar}/^{39}\text{Ar}$
995 geochronology. *Chem. Geol.* 255 (3e4), 463e466.
- 996 Ridolfi, F., Renzulli, A., Macdonald, R., Upton, B.G.J., 2006. Peralkaline syenite autoliths
997 from Kilombe volcano, Kenya Rift Valley: Evidence for subvolcanic interaction with
998 carbonatitic fluids. *Lithos* 91, 373-392.
- 999 Roberts M.B., Parfitt S.G. 1999. *Boxgrove: A Middle Pleistocene Hominid Site at Eartham*
1000 *Quarry, Boxgrove, West Sussex.* English Heritage, London.
- 1001 Roche H., Delagnes A., Brugal J-P., Feibel C., Kibunjia M., Mourre V., Texier, J-P. 1999.
1002 Early hominid stone tool production and technical skill 2.34Myr ago in West Turkana,
1003 Kenya. *Nature* 399, 57-60.
- 1004 Sharon, G., 2007. *Acheulian Large Flake Industries: Technology, Chronology, and*
1005 *Significance.* Archaeopress, Oxford (BAR International Series).
- 1006 Sherwood, R.J., Ward, S.C., Hill, A., 2002. The taxonomic status of the Chemeron temporal
1007 (KNM-BC 1). *Journal of Human Evolution* 42, 153-184.
- 1008 Stanistreet, I., McHenry, L.J., Stollhofen, H., de la Torre, I. 2018. Bed II Sequence
1009 Stratigraphic context of EF-HR and HWK EE archaeological sites, and the

- 1010 Oldowan/Acheulean succession at Olduvai Gorge, Tanzania. *Journal of Human*
1011 *Evolution* 120:19-31. doi: 10.1016/j.jhevol.2018.01.005.
- 1012 Stoenner, R.W., Oa, S., Katcoff, S., 1965. Half-lives of Argon-37 Argon-39 and Argon-42.
1013 *Science* 148 (3675), 1325.
- 1014 Torre, de la, I., 2016. The origins of the Acheulean: past and present perspectives on a major
1015 transition in human evolution. *Phil. Trans. R. Soc. B* 371, 20150245.
1016 <https://doi/0.1098/rstb.2015.0245>)
- 1017 Trauth, M.H., Maslin, M.A., Deino, A., 2005. Late Cenozoic moisture history of East Africa.
1018 *Science* 309, 2051-2053.
- 1019 Tryon, C.A., 2006. "Early" Middle Stone Age lithic technology of the Kapthurin Formation
1020 (Kenya). *Current Anthropology* 47, 367-375.
- 1021 Tryon, C.A., McBrearty, S., 2002. Tephrostratigraphy and the Acheulian to Middle Stone Age
1022 transition in the Kapthurin Formation, Kenya. *Journal of Human Evolution* 42, 211-
1023 235.
- 1024 Tryon, C.A., McBrearty, S., 2006. Tephrostratigraphy of the Bedded Tuff Member (Kapthurin
1025 Formation, Kenya) and the nature of archaeological change in the later middle
1026 Pleistocene. *Quaternary Research* 65, 492-507.
- 1027 Uribe Larrea, D., Martín-Perea, D., Díez-Martín, F., Policarpo Sánchez-Yustos, P., Domínguez-
1028 Rodrigo, M., Enrique Baquedano, E., Mabulla, A., 2017. A reconstruction of the
1029 paleolandscape during the earliest Acheulian of FLK West: The co-existence of
1030 Oldowan and Acheulian industries during lowermost Bed II (Olduvai Gorge,
1031 Tanzania). *Palaeogeography, Palaeoclimatology and Palaeoecology* 488, 50-58.
- 1032 Wendorf, F., Schild, R., 1974. *A Middle Stone Age sequence from the Central Rift Valley,*
1033 *Ethiopia.* Institute for History and Material Culture, Polish National Academy,
1034 Warsaw.
- 1035 Wilkins, J., Schoville, B.J., Brown, K.S., Chazan, M. 2012. Evidence for early hafted hunting
1036 technology. *Science* 338, 942-946.
- 1037
- 1038
- 1039
- 1040

1041 **Tables:**

1042

1043 Table 1: Ar-Ar dates

1044

1045

1046 **Figures:**

1047 Figure 1: Location maps of the Kilombe area, (a) in East Africa, (b) in the Kenya Rift Valley.

1048 Figure 2: Map of Kilombe Caldera and the southern flanks of Kilombe volcano.

1049 Figure 3: Stratigraphic overview of the two main exposure series: Kilombe Caldera and the
1050 mountain southern flank. Above: profile from Kilombe mountain to the Molo River
1051 showing sampling areas. Scale in km.1052 Figure 4: Detailed map of Kilombe Caldera localities, showing the designated sites (see Figure
1053 2 for position of this map). Background courtesy Google Earth.1054 Figure 5: Outline section of the Kilombe Caldera sediments, dating samples and
1055 archaeological/faunal localities. Inset map shows position of section line (cf Figure 4).1056 Figure 6: The upper staircase of tuffs and sediments visible in Kilombe Caldera. Arrows
1057 indicate the positions of sites GqJh13A, Oldowan, and GqJh15A, Acheulean.1058 Figure 7: Oldowan artefacts of trachyte, site GqJh13A. Left: simple core, showing
1059 detachment area of a single main flake. Right: flake, dorsal and ventral views. Scale
1060 in cm.

1061 Figure 8: Acheulean handaxe of trachyte from Kilombe Caldera site GqJh15A. Scale in cm.

1062 Figure 9: MSA obsidian points from Site GqJh3 W 200; lower view is of casts showing greater
1063 surface detail. Scale in cm.

1064

1065 **(Figures Below)**

1066



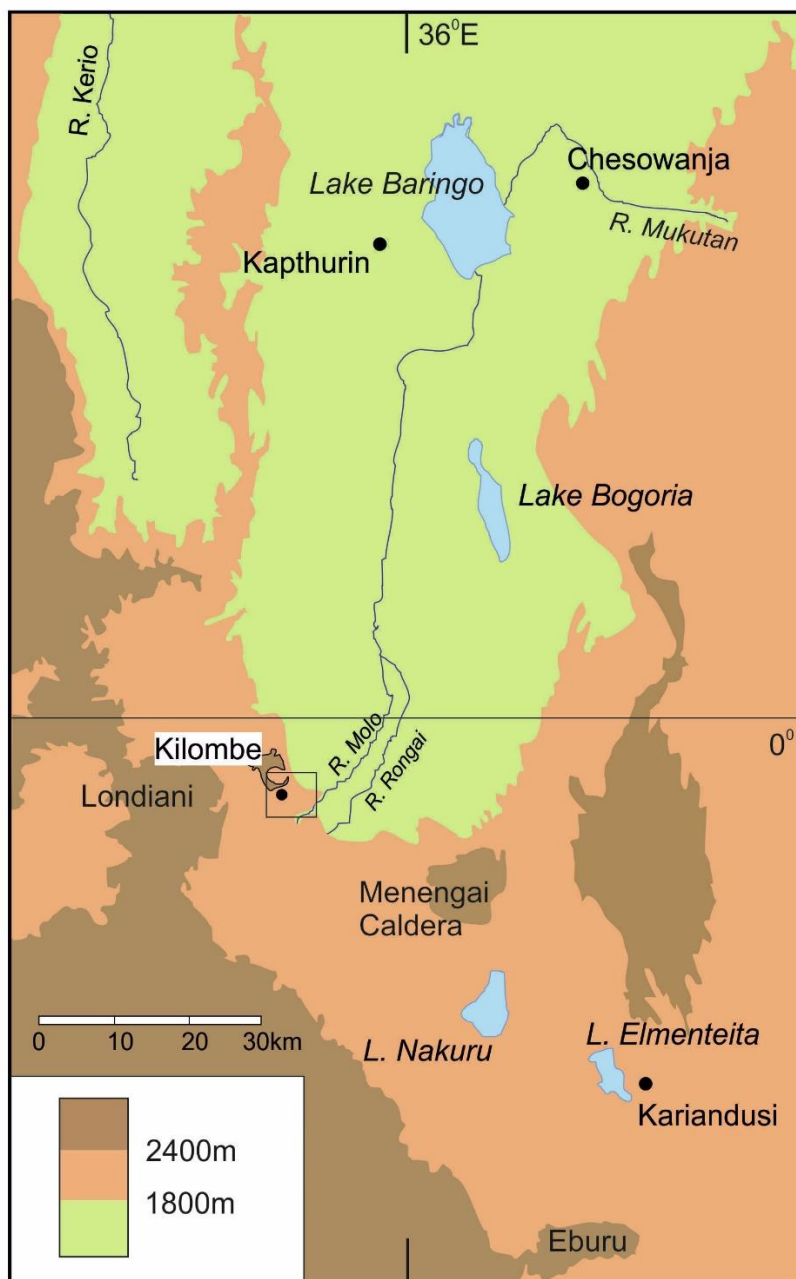
1067

1068

1069

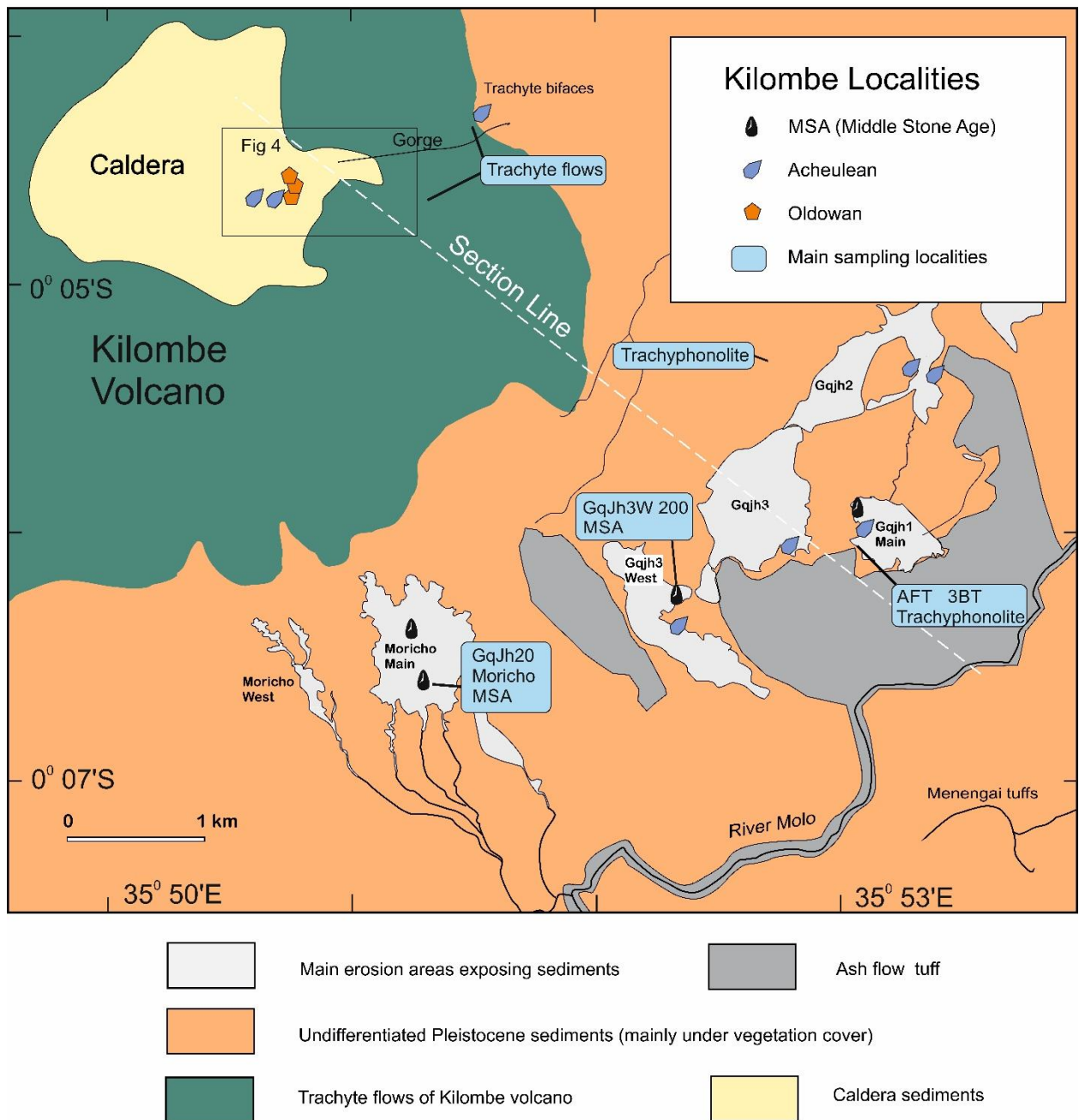
1070 Figure 1: Location maps of the Kilombe area, (a) in East Africa, (b) in the Kenya Rift Valley.

1071



1072
 1073
 1074

Figure 1: Location maps of the Kilombe area, (a) in East Africa, (b) in the Kenya Rift Valley.



1075

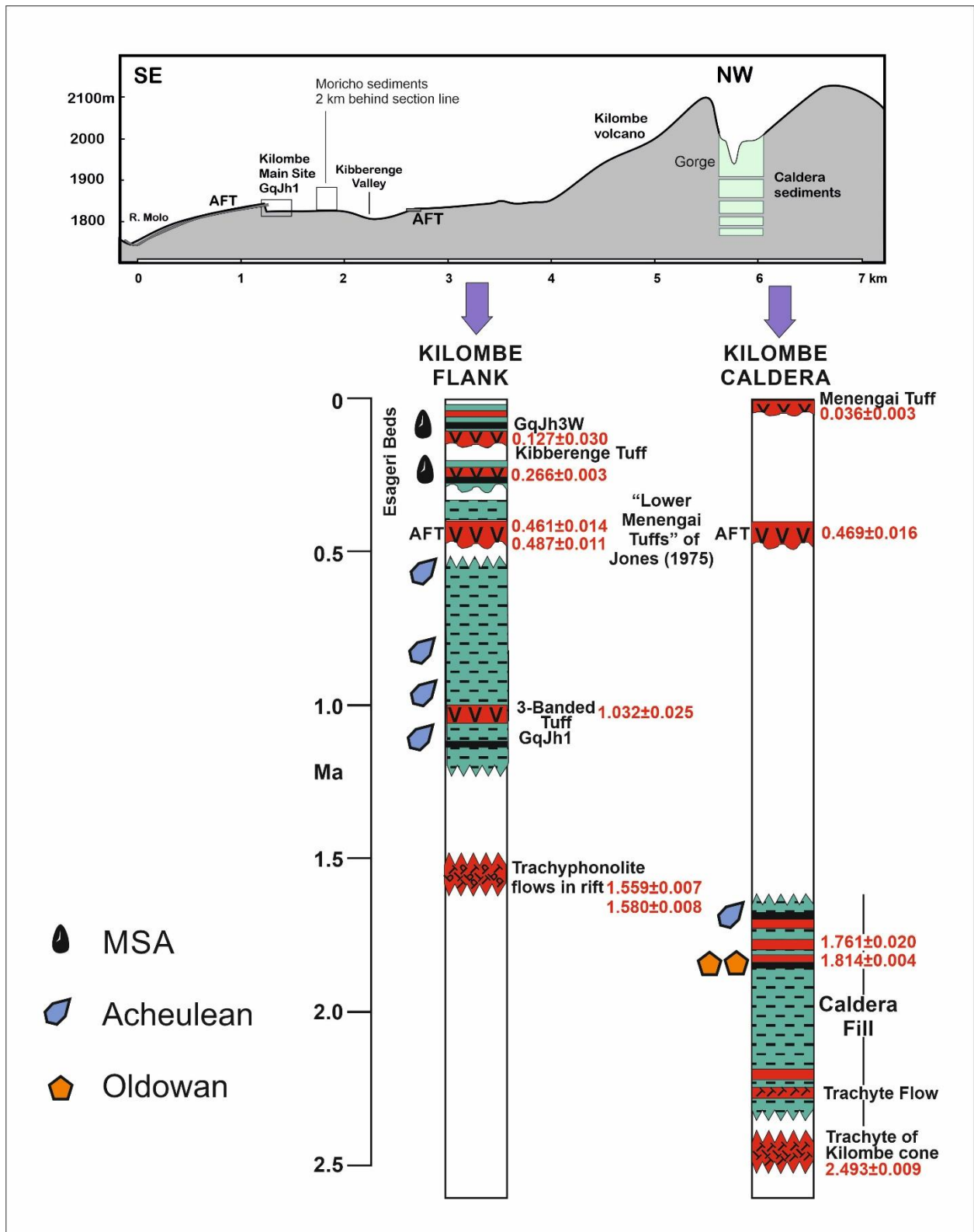
1076

1077

1078

Figure 2: Map of Kilombe Caldera and the southern flanks of Kilombe volcano.

1079



1080

1081 Figure 3: Stratigraphic overview of the two main exposure series: Kilombe Caldera and the
 1082 mountain southern flank. Above: profile from Kilombe mountain to the Molo River
 1083 showing sampling areas. Scale in km.



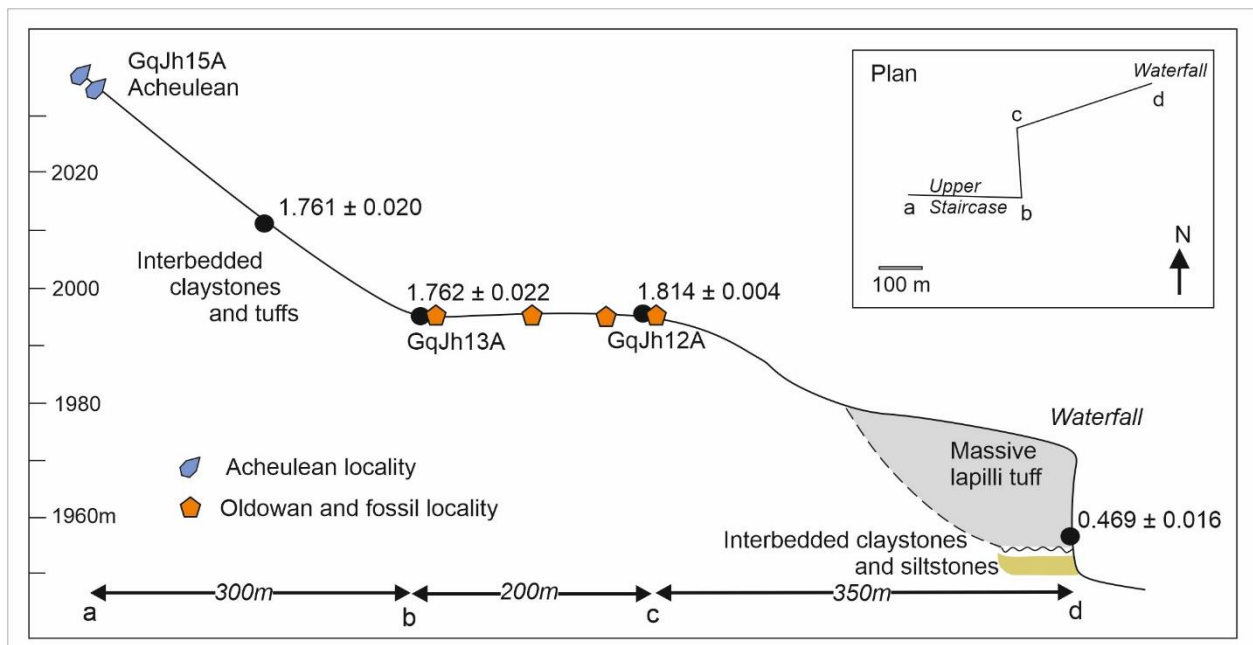
◆ Oldowan + fauna
 ◆ Early Acheulean
 ▲ Possible Early Acheulean

1084

1085

1086 Figure 4: Detailed map of Kilombe Caldera localities, showing the designated sites (see Figure
 1087 2 for position of this map). Background courtesy of Google Earth.

1088



1089

1090 Figure 5: Outline section of the Kilombe Caldera sediments, dating samples and
 1091 archaeological/faunal localities. Inset map shows position of section line (cf Figure 4).



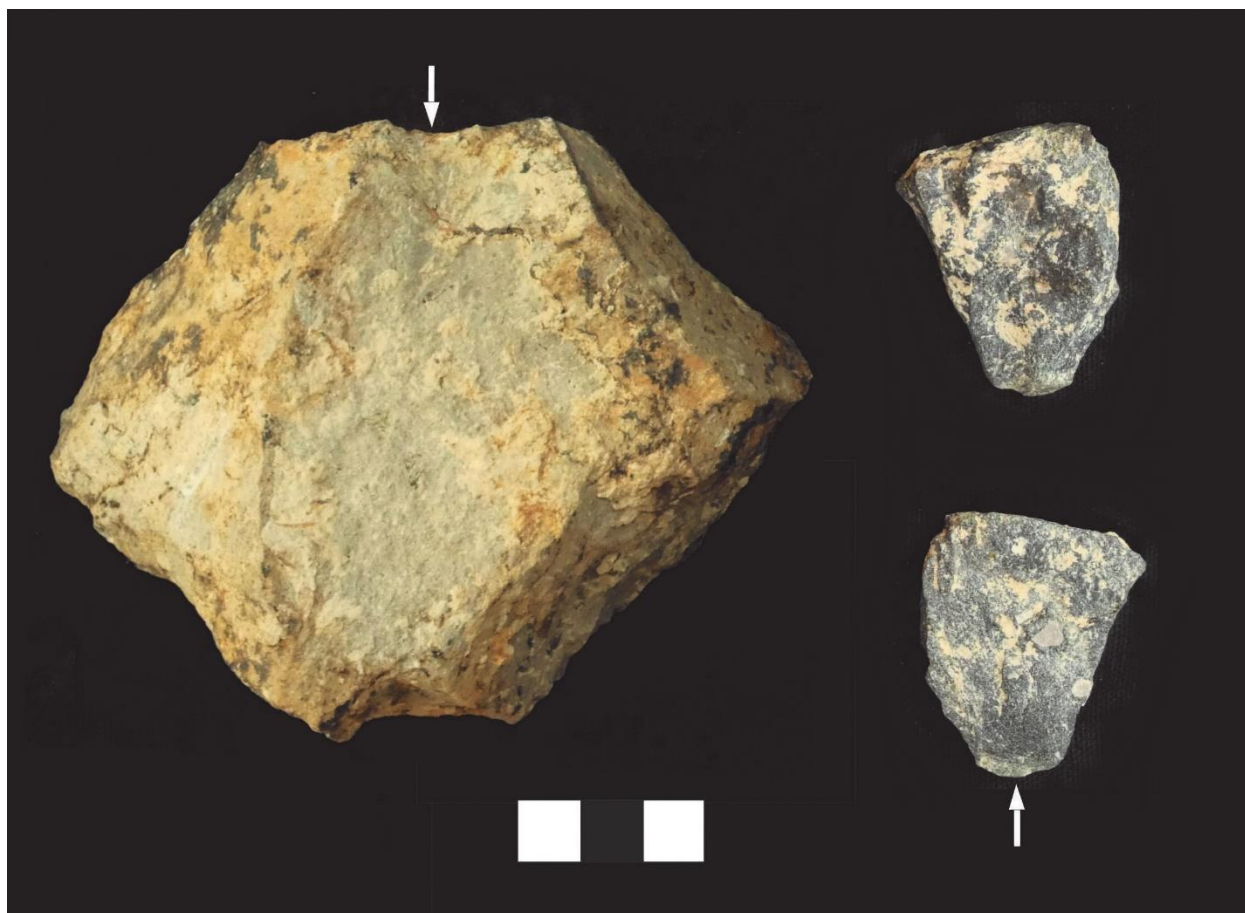
1092

1093

1094 Figure 6: The upper staircase of tuffs and sediments visible in Kilombe Caldera. Arrows

1095 indicate the positions of sites GqJh13A, Oldowan, and GqJh15A, Acheulean.

1096



1097

1098

1099

1100 Figure 7: Oldowan artefacts of trachyte, site GqJh13A. Left: simple core, showing
1101 detachment area of a single main flake. Right: flake, dorsal and ventral views. Scale
1102 in cm.

1103

1104



1105

1106 Figure 8: Acheulean handaxe of trachyte from Kilombe Caldera site GqJh15A. Scale in cm.

1107

1108



1109

1110

1111 Figure 9: MSA obsidian points from Site GqJh3 W 200; lower view is of casts showing greater
1112 surface detail. Scale in cm.